Accessible and inaccessible quantum coherence in relativistic quantum systems

Saveetha Harikrishnan,[1,*] Segar Jambulingam,[2,†] Peter P. Rohde,[3,4,‡] and Chandrashekar Radhakrishnan[5,1,§]

[1]*Centre for Quantum Science & Technology, Chennai Institute of Technology, Chennai 600069, India*

[2]*Department of Physics, Ramakrishna Mission Vivekananda College, Mylapore, Chennai 600 004, India*

[3]*Centre for Quantum Software & Information (UTS:QSI), University of Technology Sydney, Ultimo, New South Wales 2007, Australia*

[4]*Hearne Institute for Theoretical Physics, Department of Physics & Astronomy, Louisiana State University, Baton Rouge, Louisiana, United States*

[5]*Centre for Quantum Information, Communication and Computing, Indian Institute of Technology Madras, Chennai 600036, India*

(Received 12 July 2021; revised 20 December 2021; accepted 19 April 2022; published 3 May 2022)

The quantum coherence of a multipartite system is investigated when some of the parties are moving with uniform acceleration and the analysis is carried out using the single-mode approximation. Due to acceleration the quantum coherence is divided into two parts as accessible and inaccessible coherence. First we investigate tripartite systems, considering both GHZ and W states. We find that the quantum coherence of these states does not vanish in the limit of infinite acceleration, rather asymptoting to a nonzero value. These results hold for both single- and two-qubit acceleration. In the GHZ and W states the coherence is distributed as correlations between the qubits and is known as global coherence. However, quantum coherence can also exist due to the superposition within a qubit, the local coherence. To study the properties of local coherence we investigate a separable state. The GHZ state, W state, and separable states contain only one type of coherence. Next we consider the $W\bar{W}$ and star states in which both local and global coherences coexist. We find that under uniform acceleration both local and global coherence show similar qualitative behavior. Finally, we derive analytic expressions for the quantum coherence of N-partite GHZ and W states for $n < N$ accelerating qubits. We find that the quantum coherence of a multipartite GHZ state falls exponentially with the number of accelerated qubits, whereas for multipartite W states the quantum coherence decreases only polynomially. We conclude that W states are more robust to Unruh decoherence and discuss some potential applications in satellite-based quantum communication and black-hole physics.

DOI: 10.1103/PhysRevA.105.052403

I. INTRODUCTION

Entanglement is a widely studied quantum resource with applications in quantum computing [1], quantum algorithms [2–4], metrology [5], teleportation [6,7], and cryptography [8,9]. In recent times, it has become more apparent that there are several other quantum properties such as nonlocality [10], steering [11], discord [12], and coherence [13], which can also be used as a resource. Based on their relative presence, it is known that there is a hierarchy among these different resources. Of all these resources, quantum coherence is more extensively present, even when the quantum system does not have steering, entanglement, or discord. Hence an investigation of quantum coherence can provide more complete information about the "quantumness" of physical systems. Consequently, several studies were performed into quantum coherence with the aim being to understand the fundamental quantum behavior of systems. Some important investigations carried out so far are on the measurement of quantum coherence [13,14], the formulation of the resource theory of quantum coherence [15–18], the effect of external environments on coherence [19,20], and finally, the applications of quantum coherence [21–23].

Investigations in quantum information theory are generally carried out in inertial reference frames. An extension to noninertial reference frames was discussed through several works [24–27]. In this context, entanglement in noninertial frames of reference has been an important area of research [28–30]. Initial works [31] in this direction considered a family of peaked Minkowski wave packets which admits only a single Unruh mode. Later on, the entanglement of a general set of states was discussed in a multimode setting [32,33]. Though the multimode approximation is more generally valid, several studies were still carried out in the single-mode approximation [34] due to the ease of obtaining a clear analytic expression. Another approach was also available in the noninertial scenario by considering the Unruh-Dewitt detector model [35,36]. Several interesting results were obtained in the fields of black-hole physics [31,37–41], quantum error correction [42], relativistic quantum metrology [43–46], relativistic teleportation [47–50], and communication [36,51–53]. Similar studies on relativistic effects on quantum discord [54,55] have also been performed. Recent experimental advances have increased the scope of quantum technologies

*saveethah@citchennai.net

†segar@rkmvc.ac.in

‡dr.rohde@gmail.com, https://www.peterrohde.org

§chandrashekar10@gmail.com

from applications in terrestrial situations [56–58] to satellite-based space-level technologies [59–65]. Hence, we investigate quantum coherence under uniform acceleration since, compared to entanglement or other resources, it is more commonly found and can be measured more easily.

The effect of relativistic motion on quantum coherence was studied in Refs. [66–69]. In Ref. [66], the relativistic effects on the quantum coherence between a pair of Unruh-Dewitt detectors was studied. Here the authors found that, compared to entanglement, quantum coherence was more robust to Unruh decoherence. A generalization of this result to the tripartite system was performed by the authors of Ref. [68]. Both these works considered a massless scalar field. The relativistic coherence of a system of Dirac fields was considered in Ref. [69]. In our work we consider the modes of a massless scalar field and measure the coherence between different modes as well as the coherence within a mode. Here we consider a uniformly accelerating system, which can be described using a family of peaked Minkowski wave packets, and consequently, we work in the single-mode setting. We estimate the information-theoretic change in the coherence of the system using the ℓ_1 norm of coherence. For a complete study of tripartite systems, we investigate both the stochastic local operations and classical communication (SLOCC) class of states, namely, the Greenberger-Horne-Zeilinger (GHZ) and W class of states. However, these two states have only global coherence, which arises due to the correlation between qubits. For completeness sake, we investigate the relativistic effects on separable states with only local coherence, a type of quantum coherence arising due to the superposition within qubits. We also look into two different tripartite states, namely, the $W\bar{W}$ and star states in which both global and local coherence coexist.

The structure of the paper is as follows. In Sec. II we discuss the notion of relativity in the field of quantum information and also introduce the ℓ_1 norm of coherence, which is used to measure coherence in our work. The SLOCC class of states is studied in detail in Sec. III with the GHZ class and W class forming two different subsections. The separable state and an introduction to the notions of local coherence and global coherence are described in Sec. IV. The tripartite systems with both local and global coherence are analyzed in Sec. V. In Sec. VI we discuss certain applications related to satellite-based communication as well as black holes. Finally in Sec. VII we discuss our results.

II. RELATIVITY AND QUANTUM COHERENCE

To describe events independent of the inertial frame of reference, the combination of three space and one time dimension known as Minkowski space are used. For noninertial reference frames we need to use the Rindler coordinates. The Minkowski and Rindler coordinates are related to each other via a Rindler transformation. For a situation with one spatial and one time dimension (z, t), the Minkowski space-time is divided into four wedges as shown in Fig. 1. The regions F and P represent the future and the past light cones and the regions I and II are the two causally disconnected Rindler regions. The equations $|z| = t$ and $|z| = -t$ describe the future and past event horizons. For situations with one spatial and one time dimension (z, t), the world lines of uniformly accelerated observers in Minkowski coordinates correspond to a hyperbola. The two branches of the hyperbola constitute the regions I and II of the Rindler coordinates. The coordinates of the two regions are

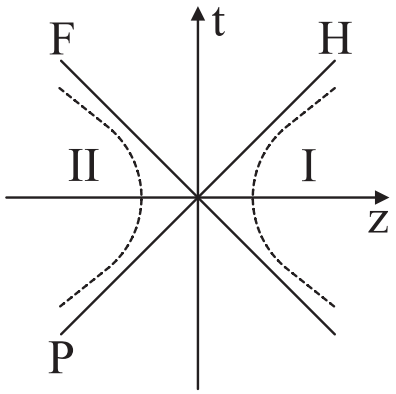

FIG. 1. The (z, t) plane of the Minkowski coordinates is divided into four regions of the Rindler coordinates. The solid lines are the future (F) and past (P) event horizons and the dashed lines are the trajectories of the uniformly accelerated observers. Here H represents the horizon.

$$\begin{aligned} t &= a^{-1}e^{a\xi}\sinh a\tau, \quad z = a^{-1}e^{a\xi}\cosh a\tau, \quad |z| < t, \\ t &= -a^{-1}e^{a\xi}\sinh a\tau, \quad z = a^{-1}e^{a\xi}\cosh a\tau, \quad |z| > t, \end{aligned} \tag{2.1}$$

where ξ is the space-like coordinate, τ is proper time, and a is acceleration.

Alice, Bob, and Charlie each have a monochromatic detector with their corresponding frequencies ω_1, ω_2, and ω_3 of a free massless scalar field in a Minkowski space-time. A maximally entangled GHZ state in the framework reads

$$\frac{|0_{\omega_1}\rangle^{\mathcal{M}}|0_{\omega_2}\rangle^{\mathcal{M}}|0_{\omega_3}\rangle^{\mathcal{M}} + |1_{\omega_1}\rangle^{\mathcal{M}}|1_{\omega_2}\rangle^{\mathcal{M}}|1_{\omega_3}\rangle^{\mathcal{M}}}{\sqrt{2}}, \tag{2.2}$$

where $|0_{\omega_i}\rangle^{\mathcal{M}}$ ($|1_{\omega_i}\rangle^{\mathcal{M}}$) is the vacuum (single-particle excitation) state of frequency ω_i in Minkowski space. Initially, when all three parties are in inertial frames then $|0_{\omega_1}\rangle^{\mathcal{M}}$, $|0_{\omega_2}\rangle^{\mathcal{M}}$, and $|0_{\omega_3}\rangle^{\mathcal{M}}$ are their respective ground states. Their excited states can be obtained by applying their corresponding Minkowski creation operators as follows:

$$|n_{\omega_i}\rangle^{\mathcal{M}} = \frac{(\hat{a}^{\dagger}_{\omega_i})^n}{\sqrt{n!}}|0_{\omega_i}\rangle^{\mathcal{M}}. \tag{2.3}$$

If Charlie starts moving with uniform acceleration, the wave function becomes highly delocalized in space and the quantum state corresponding to the frequency ω_3 can be specified using Rindler or Unruh coordinates [32]. In both the Rindler and Unruh basis, the initial Minkowski space is divided into two regions which are casually disconnected from each other. Let Ω be the dimensionless Rindler frequency and the Unruh modes are also sharply peaked at the same frequency. Using an analytic continuation argument, it was shown [32] that the Unruh mode is a purely positive frequency linear combination of the Minkowski modes. However, the

definition of positive frequency in the Rindler mode differs from the positive frequency definition on the Minkowski mode. So we can relate the Minkowski and the Rindler modes via the Unruh modes. The field in each of these three bases are expanded as follows:

$$\begin{aligned}\phi &= \int_0^\infty (a_{\omega,\mathcal{M}} u_{\omega,\mathcal{M}} + a^\dagger_{\omega,\mathcal{M}} u^*_{\omega,\mathcal{M}})\, d\omega \\ &= \int_0^\infty (A_{\Omega,R} u_{\Omega,R} + A^\dagger_{\Omega,R} u^*_{\Omega,R} + A_{\Omega,L} u_{\Omega,L} + A^\dagger_{\Omega,L} u^*_{\Omega,L})\, d\Omega \\ &= \int_0^\infty (b_{\Omega,\mathrm{I}} u_{\Omega,\mathrm{I}} + b^\dagger_{\Omega,\mathrm{I}} u^*_{\Omega,\mathrm{I}} + b_{\Omega,\mathrm{II}} u_{\Omega,\mathrm{II}} + b^\dagger_{\Omega,\mathrm{II}} u^*_{\Omega,\mathrm{II}})\, d\Omega,\end{aligned} \tag{2.4}$$

where $a_{\omega,\mathcal{M}}$ is the Minkowski annihilation operator, $A_{\Omega,R}\&A_{\Omega,L}$ are the Unruh annihilation operator for the right and left regions, and $b_{\Omega,\mathrm{I}}\&b_{\Omega,\mathrm{II}}$ are the Rindler annihilation operators in the I and II regions. The operators obey the bosonic commutation relations $[a_{\omega_1,\mathcal{M}}, a^\dagger_{\omega_2,\mathcal{M}}] = \delta_{\omega_1\omega_2}$, $[A_{\Omega_1,R}, A^\dagger_{\Omega_2,R}] = [A_{\Omega_1,L}, A^\dagger_{\Omega_2,L}] = \delta_{\Omega_1\Omega_2}$, and $[b_{\Omega_1,\mathrm{I}}, b^\dagger_{\Omega_2,\mathrm{I}}] = [b_{\Omega_1,\mathrm{II}}, b^\dagger_{\Omega_2,\mathrm{II}}] = \delta_{\Omega_1\Omega_2}$. For the Unruh mode, the commutator between operators in the R and L regions vanish. Similarly, the commutator between the operators in regions I and II vanish. The creation and annihilation operators of the Minkowski and Unruh bases do not mix and hence we have $|0\rangle_M = |0\rangle_U = \prod_\Omega |0_\Omega\rangle_U$. But the state $|0\rangle_U$ does not coincide with the Rindler vacuum and we have

$$|0_\Omega\rangle_U = \sum_N \frac{\tanh^n r_\Omega}{\cosh r_\Omega} |n_\Omega\rangle_\mathrm{I} |n_\Omega\rangle_\mathrm{II}. \tag{2.5}$$

Here $|n_\Omega\rangle_\mathrm{I}$ is the nth excited state of the Rindler I vacuum state $|0_\Omega\rangle_\mathrm{I}$.

We consider a wave packet which is narrowly peaked in Ω and for this the Unruh and Rindler commutators read $[A_{\Omega,R}, A^\dagger_{\Omega,R}] = [A_{\Omega,L}, A^\dagger_{\Omega,L}] = 1$ and $[b_{\Omega,\mathrm{I}}, b^\dagger_{\Omega,\mathrm{I}}] = [b_{\Omega,\mathrm{II}}, b^\dagger_{\Omega,\mathrm{II}}] = 1$. Under these ideal conditions, the most general creation operator of a purely positive Minkowski frequency can be written as

$$a^\dagger_{\Omega,U} = q_L A^\dagger_{\Omega,L} + q_R A^\dagger_{\Omega,R}. \tag{2.6}$$

Here the factors q_R and q_L are complex numbers with $|q_R|^2 + |q_L|^2 = 1$. Under these conditions we have

$$\begin{aligned}a^\dagger_{\Omega,U}|0_\Omega\rangle_U &= \sum_{n=0}^\infty \frac{\tanh^n r_\Omega}{\cosh r_\Omega} \left(\frac{\sqrt{n+1}}{\cosh r_\Omega}\right) \left|\Phi^n_\Omega\right\rangle, \\ \left|\Phi^n_\Omega\right\rangle &= q_L |n_\Omega\rangle_\mathrm{I} |(n+1)_\Omega\rangle_\mathrm{II} + q_R |(n+1)_\Omega\rangle_\mathrm{I} |n_\Omega\rangle_\mathrm{II},\end{aligned} \tag{2.7}$$

where, in general, we consider $q_R = 1$ and $q_L = 0$. Let us consider a Minkowski smearing function which is a Gaussian in $\ln(\omega l)$,

$$f(\omega) = \left(\frac{\lambda}{\pi\omega^2}\right)^{1/4} \exp\left\{\frac{-1}{2}\lambda[\ln(\omega/\omega_0)]^2\right\} (\omega/\omega_0)^{-i\mu}, \tag{2.8}$$

When the uniformly accelerated particle has the above smearing function and has negligible overlap with the other states, then it is well approximated by a single Unruh frequency. Thus we use this monochromatic wave approximation in our investigation. Under this condition, the Minkowski and Rindler modes can be connected via the relations

$$\begin{aligned}\hat{a}^\dagger_{\omega_3} &= \hat{b}^\dagger_{\Omega_3\mathrm{I}} \cosh r - \hat{b}_{\Omega_3\mathrm{II}} \sinh r = \hat{S}_{\Omega_3} \hat{b}^\dagger_{\Omega_3\mathrm{I}} \hat{S}^\dagger_{\Omega_3}, \\ \hat{a}_{\omega_3} &= \hat{b}_{\Omega_3\mathrm{I}} \cosh r - \hat{b}^\dagger_{\Omega_3\mathrm{II}} \sinh r = \hat{S}_{\Omega_3} \hat{b}_{\Omega_3\mathrm{I}} \hat{S}^\dagger_{\Omega_3},\end{aligned} \tag{2.9}$$

where

$$\hat{S}_\Omega(r) = \exp[r(\hat{b}^\dagger_{\Omega\mathrm{I}} \hat{b}^\dagger_{\Omega\mathrm{II}} - \hat{b}_{\Omega\mathrm{I}} \hat{b}_{\Omega\mathrm{II}})]. \tag{2.10}$$

Here the operator ($\hat{S}$) effecting the transformation from Minkowski coordinates to Rindler coordinates is structurally identical to the two-mode squeezing operator

$$\hat{S}(\zeta) = \exp(\zeta^* ab - \zeta a^\dagger b^\dagger), \tag{2.11}$$

in the quantum optics context. Hence for a noninertial observer, the single-mode Minkowski vacuum becomes a two-mode squeezed state in the Rindler vacuum

$$\begin{aligned}|0_\omega\rangle^\mathcal{M} &= \hat{S}_{\Omega_3}(r)(|0\rangle_\mathrm{I} \otimes |0\rangle_\mathrm{II}) \\ &= \frac{1}{\cosh r} \sum_{n=0}^\infty \tanh^n r |n_\Omega\rangle_\mathrm{I} |n_\Omega\rangle_\mathrm{II},\end{aligned} \tag{2.12}$$

where $\cosh r = (1 - e^{-2\pi\Omega})^{-1/2}$ and $\Omega = |\omega|c/a$. The factors ω and c are the wave vector and velocity of light, respectively. Here $|n_\Omega\rangle_\mathrm{I}$ and $|n_\Omega\rangle_\mathrm{II}$ are the mode decompositions in Rindler regions I and region II, respectively. For the single-particle excitation state we have

$$\begin{aligned}|1_\omega\rangle^\mathcal{M} &= \hat{a}^\dagger_{\omega_3} \left|0_{\omega_3}\right\rangle^\mathcal{M} = \hat{S}_{\Omega_3}(r) \hat{b}^\dagger_{\Omega_3\mathrm{I}} (|0\rangle_\mathrm{I} \otimes |0\rangle_\mathrm{II}) \\ &= \frac{1}{\cosh^2 r} \sum_{n=0}^\infty \sqrt{n+1} \tanh^n r |(n+1)_\Omega\rangle_\mathrm{I} |n_\Omega\rangle_\mathrm{II}.\end{aligned}$$

We observe that, due to the squeezing behavior of a noninertial observer, a single Minkowski mode can be written as a superposition of two Rindler modes. Consequently, there exists coherence between the two Rindler modes. Since these two modes are not causally connected, this coherence cannot be experimentally observed. Actually, there is no new coherence created in the system.

To illustrate this let us consider a tripartite system with Alice and Bob at rest and Charlie moving with constant acceleration. The coherence shared by Charlie with Alice and Bob is split into two parts. One part remains in Rindler mode I and can be experimentally observed, which we call the *accessible coherence*. The other part of the coherence, which is shared with Rindler mode II, cannot be measured, which we refer to as *inaccessible coherence*. This inaccessible coherence quantifies the decrease in coherence due to relativistic effects. A schematic diagram explaining the accessible and inaccessible coherence is shown in Fig. 2.

In a tripartite state when two qubits are accelerated the vacuum ($|000\rangle$) and excited ($|111\rangle$) states can be expressed as

$$\begin{aligned}|000\rangle_{\mathrm{ABC}} &= |0\rangle \otimes |0\rangle \otimes |0\rangle \\ &\xrightarrow{\text{accl}} |0_{\omega_1}\rangle \otimes \left[\hat{S}_{\Omega_2}(r_2)\left(|0_{\Omega_2}\rangle_{\mathrm{I}} \otimes |0_{\Omega_2}\rangle_{\mathrm{II}}\right)\right] \otimes \left[\hat{S}_{\Omega_3}(r_1)\left(|0_{\Omega_3}\rangle_{\mathrm{I}} \otimes |0_{\Omega_3}\rangle_{\mathrm{II}}\right)\right] \\ &= |0\rangle \otimes \frac{1}{\cosh r_2}\left[\sum_{m=0}^{\infty} \tanh^m r_2 |m\rangle_{\mathrm{I}}|m\rangle_{\mathrm{II}}\right] \otimes \left[\frac{1}{\cosh r_1}\sum_{n=0}^{\infty} \tanh^n r_1 |n\rangle_{\mathrm{I}}|n\rangle_{\mathrm{II}}\right], \end{aligned} \tag{2.13}$$

$$\begin{aligned}|111\rangle_{\mathrm{ABC}} &= |1\rangle \otimes |1\rangle \otimes |1\rangle \\ &\xrightarrow{\text{accl}} |1_{\omega_1}\rangle \otimes \left[\hat{S}_{\Omega_2}(r_2)\hat{b}^{\dagger}_{\Omega_2\mathrm{I}}\left(|0_{\Omega_2}\rangle_{\mathrm{I}} \otimes |0_{\Omega_2}\rangle_{\mathrm{II}}\right)\right] \otimes \left[\hat{S}_{\Omega_3}(r_1)\hat{b}^{\dagger}_{\Omega_3\mathrm{I}}\left(|0_{\Omega_3}\rangle_{\mathrm{I}} \otimes |0_{\Omega_3}\rangle_{\mathrm{II}}\right)\right] \\ &= |1\rangle \otimes \left[\frac{1}{\cosh^2 r_2}\sum_{m=0}^{\infty} \sqrt{m+1}\tanh^m r_2 |m+1\rangle_{\mathrm{I}}|m\rangle_{\mathrm{II}}\right] \otimes \left[\frac{1}{\cosh^2 r_1}\sum_{n=0}^{\infty} \sqrt{n+1}\tanh^n r_1 |n+1\rangle_{\mathrm{I}}|n\rangle_{\mathrm{II}}\right]. \end{aligned} \tag{2.14}$$

The modes I and II correspond to the two causally disconnected regions in Rindler coordinates of Minkowski space. Hence mode II is physically inaccessible to Alice, Bob, and Charlie and is partially traced out. For an inertial observer, a quantum system in Minkowski space-time is independent of the nature of the observer. However, when the observer is moving with constant acceleration, they perceive a thermal bath with temperature proportional to acceleration. This thermal bath is made up of Rindler particles which are associated with the vacuum state of Minkowski space. Due to this thermal bath, the observer perceives decoherence of the quantum system, a phenomenon known as Unruh decoherence.

Quantum coherence is, in general, measured as the distance between the quantum state under consideration and the closest incoherent state in the same basis. Several measures of quantum coherence [13,14,70,71] were presented, but in the first work on quantum coherence by Baumgratz, Cramer, and Plenio [13] two measures were introduced corresponding to the entropic class and geometric class of measures. The relative entropy-based measure of quantum coherence belongs to the entropic class and the ℓ_1 norm of coherence to the geometric class. Here we use the ℓ_1 norm of quantum coherence, defined as

$$C_{l_1}(\hat{\rho}, \hat{\rho}_d) = \|\hat{\rho} - \hat{\rho}_d\|_{l_1} = \sum_{i \neq j} |\hat{\rho}_{i,j}|, \tag{2.15}$$

where $\hat{\rho}$ is a given density matrix and $\hat{\rho}_d$ is the associated decohered density matrix defined as

$$\hat{\rho}_d = \sum_i \hat{\rho}_{i,i} |i\rangle\langle i|. \tag{2.16}$$

We can observe that this is equivalent to the sum of the off-diagonal elements of the density matrix. Using interference fringes, the quantum coherence of a physical system can be measured using the robustness of coherence [72], a measure introduced in Ref. [73]. In Ref. [74] it was shown that, for a pure state, the robustness of the coherence measure is equal to the ℓ_1 norm of coherence. Hence the ℓ_1 norm of coherence can be directly obtained from the interference fringes, providing a method to compare theoretical results with experimental data.

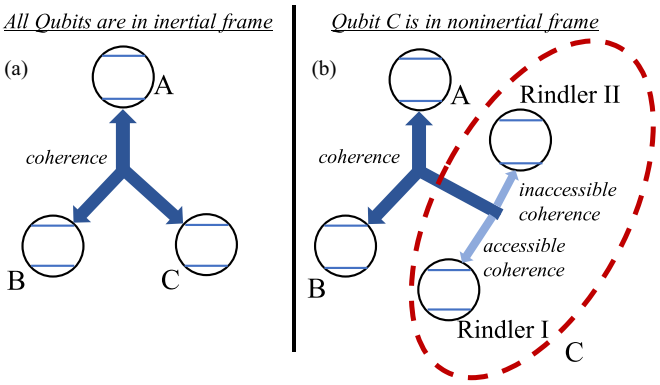

FIG. 2. A schematic diagram of coherence in tripartite is shown where the circles labeled A, B, and C represent the qubit and the blue arrow between them represents the coherence. Panel (a) contains the coherence in a tripartite system when all the qubits are in inertial frame. Panel (b) contains the coherence in the tripartite system when qubit C is under acceleration. Here qubit C enclosed by the red ellipse with dashed boundary line is split into two Rindler modes I and II. Consequently, the coherence shared by qubit C also is split into two parts. The coherence shared with C of Rindler mode I is the accessible coherence and the coherence shared with C of Rindler mode II is the inaccessible coherence. The lighter shades of blue for the accessible and inaccessible coherence represents their relative strength to the coherence initially present with C and shown in panel (a).

III. RELATIVISTIC EFFECTS IN THE SLOCC CLASS OF STATES

Based on the local operations and classical communication (LOCC), tripartite-entangled quantum states can be divided into two distinct classes, namely the GHZ class and the W class. The entanglement distribution is different in these two class of states. In a GHZ state all the entanglement vanishes even with the loss of a single qubit, whereas in a W state a finite amount of entanglement is always present even when we loose a single qubit. The coherence of these class of states in inertial frames was discussed in detail in Ref. [20]. We extend upon this by investigating the coherence when some of the qubits of the tripartite system are in a noninertial reference frame. In particular, we probe the loss of coherence due to the acceleration of qubits.

A. GHZ class

A GHZ state is maximally entangled and so the loss of just a single qubit results in the complete loss of entanglement and coherence. The general form of a tripartite GHZ state is

$$|\mathrm{GHZ}\rangle_{\mathrm{ABC}} = \cos\theta|000\rangle_{\mathrm{ABC}} + \sin\theta|111\rangle_{\mathrm{ABC}}, \tag{3.1}$$

where $\theta \in [0, 2\pi)$ is a parameter generalizing the GHZ state via the bias between the two basis states. On accelerating qubit C its Minkowski modes are replaced with their corresponding Rindler modes and the tripartite states become

$$|\mathrm{GHZ}\rangle_{\mathrm{ABC}} = \frac{1}{\cosh r}\sum_{n=0}^{\infty}\tanh^n r\Big[\cos\theta|00\rangle|n\rangle_{\mathrm{I}}|n\rangle_{\mathrm{II}} + \frac{\sqrt{n+1}}{\cosh r}\sin\theta|11\rangle|n+1\rangle_{\mathrm{I}}|n\rangle_{\mathrm{II}}\Big]. \tag{3.2}$$

Here, $|00\rangle|n\rangle_{\mathrm{I}}|n\rangle_{\mathrm{II}}$ and $|11\rangle|n+1\rangle_{\mathrm{I}}|n\rangle_{\mathrm{II}}$ refer to the quantum state in which the Minkowski modes of the first two qubits are $|ab\rangle$ and the Rindler modes corresponding to the third qubit is as $|c\rangle_{\mathrm{I}}|c\rangle_{\mathrm{II}}$. We know that the modes from the Rindler I and II regions are not causally connected, so we can trace out the modes corresponding to Rindler region II and the density matrix of the state with Alice, Bob, and Charlie reduces to

$$\hat{\rho}_{\mathrm{GHZ}} = \frac{1}{\cosh^2 r}\sum_{n=0}^{\infty}\tanh^{2n} r\Big[\cos^2\theta|00n\rangle\langle 00n| + \cos\theta\sin\theta\frac{\sqrt{n+1}}{\cosh r}(|00n\rangle\langle 11n+1|+|11n+1\rangle\langle 00n|) + \frac{n+1}{\cosh^2 r}\sin^2\theta|11n+1\rangle\langle 11n+1|\Big]. \tag{3.3}$$

The total coherence in the generalized GHZ state is calculated using the ℓ_1-norm measure of coherence. The sum of the off-diagonal elements of Eq. (3.3) is

$$C(\hat{\rho}) = \frac{2\sin\theta\cos\theta}{\cosh^3 r}\sum_{n=0}^{\infty}\sqrt{n+1}\tanh^{2n} r. \tag{3.4}$$

Using the trigonometric identities,

$$\sum_{n=0}^{\infty}\tanh^{2n} r = \cosh^2 r,$$

$$\sum_{n=0}^{\infty}(n+1)\tanh^{2n} r = \cosh^4 r, \tag{3.5}$$

and the polylogarithm function

$$\mathrm{Li}_{-1/2}(z) = \sum_{n=0}^{\infty}\sqrt{n+1}(\tanh^2 r)^{n+1}, \tag{3.6}$$

where the polylogarithm function is defined as

$$\mathrm{Li}_n(z) \equiv \sum_{k=1}^{\infty}\frac{z^k}{k^n} = \frac{z}{1^n} + \frac{z^2}{2^n} + \frac{z^3}{3^n} + \cdots, \tag{3.7}$$

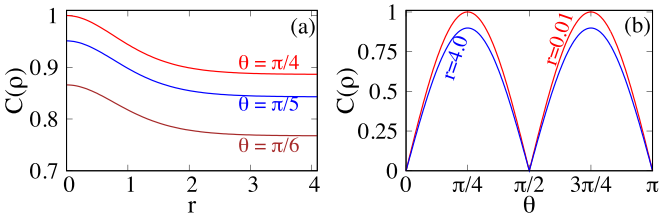

FIG. 3. The variation of coherence in a noninertial frame of reference is studied for a GHZ state under the variation of (a) the acceleration parameter r and (b) the generalization parameter θ.

the total coherence of a GHZ state when one of the qubits is in a noninertial frame can be expressed as

$$C(\hat{\rho}) = 2\sin\theta\cos\theta\frac{\mathrm{Li}_{-1/2}(\tanh^2 r)}{\sinh^2 r\,\cosh r}. \tag{3.8}$$

When Charlie's qubit is not accelerated (i.e., the $r \to 0$ limit) the corresponding quantum coherence is

$$C(\hat{\rho}) = 2\cos\theta\sin\theta. \tag{3.9}$$

The variation of quantum coherence as a function of the acceleration parameter r is shown in Fig. 3(a) for different θ values. From the plot for any given value of θ we notice that quantum coherence has a maximum value when $r = 0$, corresponding to the situation where Charlie's qubit has not yet been accelerated. The coherence then decreases with increase in r and saturates to a finite value. The decrease in coherence due to uniform acceleration is because some part of it becomes inaccessible as it lies in a causally disconnected region. The saturation value depends on the value of coherence in the inertial frame ($r = 0$). Hence, the higher the value of the coherence in the inertial frame, the higher the saturation value of coherence in the noninertial frame.

In Fig. 3(b), we study the change of the quantum coherence as a function of the generalization parameter θ for different values of the acceleration parameter r. The coherence is maximum at $\theta = (2n+1)\pi/4$ where $n \in \mathbb{Z}$ and is zero at $\theta = n\pi/2$, but the maximum value depends on the value of r.

To study the situation, when more than one party is under acceleration, we consider the setting where both Bob's and Charlie's qubits are being accelerated. The quantum state when two qubits are accelerated is

$$|\mathrm{GHZ}\rangle = \frac{1}{\cosh r_1}\frac{1}{\cosh r_2}\sum_{n,m=0}^{\infty}\tanh^n r_1\tanh^m r_2\Big[\cos\theta|0\rangle|m\rangle_{\mathrm{I}} \times |m\rangle_{\mathrm{II}}|n\rangle_{\mathrm{I}}|n\rangle_{\mathrm{II}} + \frac{\sqrt{m+1}}{\cosh r_2}\frac{\sqrt{n+1}}{\cosh r_1}\sin\theta \times |1\rangle|m+1\rangle_{\mathrm{I}}|m\rangle_{\mathrm{II}}|n+1\rangle_{\mathrm{I}}|n\rangle_{\mathrm{II}}\Big], \tag{3.10}$$

where the pairs (r_2, m) and (r_1, n) are the acceleration parameter and mode corresponding to Bob's and Charlie's qubits, respectively. To construct the density matrix we first trace out the contributions from the causally disconnected Rindler II

mode

$$\hat{\rho} = \frac{1}{\cosh^2 r_1 \cosh^2 r_2} \sum_{n=0}^{\infty}\sum_{m=0}^{\infty} \tanh^{2n} r_1 \tanh^{2m} r_2 \Big[\cos^2\theta |0\rangle|m\rangle|n\rangle\langle 0|\langle m|\langle n| + \frac{\sqrt{m+1}\sqrt{n+1}}{\cosh r_1 \cosh r_2} \cos\theta \sin\theta$$
$$\times (|0\rangle|m\rangle|n\rangle\langle 1|\langle m+1|\langle n+1| + |1\rangle|m+1\rangle|n+1\rangle\langle 0|\langle m|\langle n|) + \frac{(m+1)(n+1)}{\cosh^2 r_1 \cosh^2 r_2} \sin^2\theta$$
$$\times |1\rangle|m+1\rangle|n+1\rangle\langle 1|\langle m+1|\langle n+1| \Big], \tag{3.11}$$

From the density matrix in Eq. (3.11) and using the ℓ_1-norm measure we can determine the total quantum coherence of the GHZ state when both Bob's and Charlie's qubits are accelerated

$$C(\hat{\rho}) = 2\sin\theta\cos\theta \frac{\mathrm{Li}_{-1/2}(\tanh^2 r_1)}{\sinh^2 r_1 \cosh r_1} \frac{\mathrm{Li}_{-1/2}(\tanh^2 r_2)}{\sinh^2 r_2 \cosh r_2}, \tag{3.12}$$

where we find to be a product of two polylogarithm functions, one each corresponding to Bob's and Charlie's qubits. If Bob and Charlie have the same acceleration, which would translate to $r_1 = r_2 = r$, the coherence would then be

$$C(\hat{\rho}) = 2\sin\theta\cos\theta \left[\frac{\mathrm{Li}_{-1/2}(\tanh^2 r)}{\sinh^2 r \cosh r}\right]^2. \tag{3.13}$$

The variation of quantum coherence with the parameters r_1 and r_2 corresponding to Bob's and Charlie's acceleration is shown through the contour plots in Fig. 4. The contour plots Figs. 4(a), 4(b), and 4(c) correspond to θ of $\pi/4$, $\pi/5$, and $\pi/6$, respectively. We find that, with the increase in r_1 and r_2, the coherence decreases and saturates to a finite value. The maximal value and saturation value of coherence are dependent on the value of θ the parameter generalizing the GHZ state.

In the literature, the most commonly discussed GHZ state is $(|000\rangle + |111\rangle)/\sqrt{2}$, corresponding to the generalized GHZ state with $\theta = \pi/4$, which has quantum coherence

$$C(\hat{\rho}) = \frac{\mathrm{Li}_{-1/2}(\tanh^2 r)}{\sinh^2 r \cosh r},$$
$$C(\hat{\rho}) = \frac{\mathrm{Li}_{-1/2}(\tanh^2 r_1)}{\sinh^2 r_1 \cosh r_1} \frac{\mathrm{Li}_{-1/2}(\tanh^2 r_2)}{\sinh^2 r_2 \cosh r_2}. \tag{3.14}$$

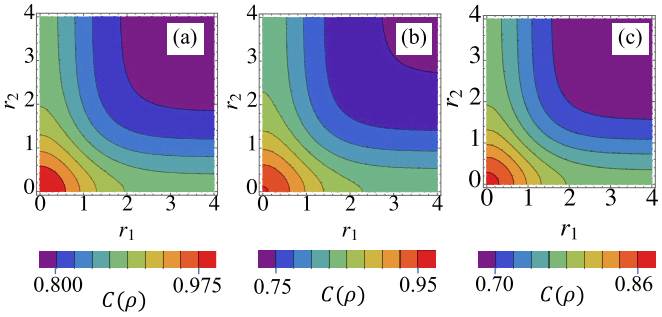

FIG. 4. The variation of quantum coherence of GHZ state with both r_1 and r_2 is shown for (a) $\theta = \pi/4$, (b) $\theta = \pi/5$, and (c) $\theta = \pi/6$, respectively.

Finally, we note that the two-qubit-reduced density matrices corresponding to the GHZ state are diagonal in nature and hence are incoherent. Thus all the coherences in the GHZ state are genuinely multipartite in nature and the loss of even one qubit removes all the coherence in the system.

In Ref. [31], the authors considered a two-qubit system of which one qubit is moving with a constant acceleration. The entanglement of the bipartite system vanished in the infinite acceleration limit. It is well known that entanglement is just one of the different types of quantum correlations. Out of the different quantifiers of quantum correlations, quantum discord measures the total quantum correlations in the system. A study of quantum discord in a relativistic system [54] shows that the total quantum correlations does not vanish in the infinite acceleration limit. Hence a bipartite system in the infinite acceleration limit has quantum correlations beyond the entanglement type. An investigation on accelerating tripartite systems was carried out in Ref. [75], where the GHZ and W states were characterized using the π-tangle measure of entanglement. The entanglement of the tripartite system did not go to zero in the infinite acceleration limit, rather it showed a decrease initially and then attained a saturation value. This is in stark contrast to the behavior of the bipartite entanglement. In Ref. [75] it was suggested that the incomplete definition of π tangle could be the reason as to why the tripartite entanglement shows a different qualitative behavior when compared to the bipartite entanglement as measured in Ref. [31]. Through the present work we observe that the quantum coherence of the GHZ state is qualitatively similar to the change in its tripartite entanglement. But here the saturation is due to the nonvanishing behavior of local quantum correlations. However, for quantum coherence, the ℓ_1 norm measures the entire quantum coherence and the saturation value is a physical feature of the system. In the case of entanglement, the saturation value may not be an actual physical feature since π tangle is inadequate to measure entanglement.

Next we can consider the three-qubit GHZ state given in Eq. (2.2) in which two qubits are under uniform acceleration. The GHZ state can be rewritten as $(|\mathbf{00}\rangle + |\mathbf{11}\rangle)/\sqrt{2}$, where $|\mathbf{0}\rangle = |00\rangle$ and $|\mathbf{1}\rangle = |11\rangle$ are redundantly encoded logical qubits. Since the GHZ state can be written in terms of the Bell state, we would expect the coherences of both these states to be equal. However, the coherence of the GHZ state when the logical qubit is accelerated is,

$$C_{\ell_1} = [\mathrm{Li}_{-1/2}(\tanh^2 r)/(\sinh^2 r \cosh r)]^2, \tag{3.15}$$

which implies that $C(|\psi_{\mathrm{Bell}}\rangle) \neq C(|\psi_{\mathrm{GHZ}}\rangle)$ is a relativistic system. This is because in the GHZ state, the logical

noninertial qubit is bigger than the regular qubit considered in the Bell state. So we find that the quantum coherence coupled with uniform acceleration helps in distinguishing between Bell states and GHZ states.

B. *W* class

The W states exhibit nonmaximal multipartite entanglement, which is not locally equivalent to GHZ-type entanglement, and may therefore be considered a distinct entanglement class. Unlike GHZ states, W states with large numbers of qubits are highly robust against qubit loss. The generalized form of the tripartite W state is

$$|W\rangle_g = \sin\theta\cos\phi|100\rangle + \sin\theta\sin\phi|010\rangle + \cos\theta|001\rangle, \tag{3.16}$$

where $\theta = [0, \pi]$ and $\phi = [0, 2\pi)$ are the parameters generalzing the W state.

First, let us consider the situation when only one qubit is in a noninertial frame of reference. Towards this end, we consider the situation when Charlie's qubit is in a noninertial frame while Alice and Bob's qubits are in an inertial frame. Naturally the Minkowski modes of Charlie's qubit are replaced by their corresponding Rindler modes. It is well known that the Minkowski region can be divided into two causally disconnected Rindler modes. So we trace out the second Rindler region from the quantum state since it is inaccessible for measurement. The total quantum coherence is then measured using the ℓ_1 norm of coherence

$$C(\hat{\rho}) = 2\sin\theta\cos\theta(\sin\phi + \cos\phi)\frac{\mathrm{Li}_{-1/2}(\tanh^2 r)}{\sinh^2 r\,\cosh r} + 2\sin^2\theta\sin\phi\cos\phi. \tag{3.17}$$

To understand the relativistic effects on a quantum state with bipartite distribution, we compute the reduced density matrices corresponding to the W state. Here, we can trace out either Alice or Bob's qubit and the quantum coherence corresponding to the reduced state is

$$C(\hat{\rho}_{BC}) = C(\hat{\rho}_{AC}) = 2\sin\theta\cos\theta\sin\phi\frac{\mathrm{Li}_{-1/2}(\tanh^2 r)}{\sinh^2 r\cosh r}. \tag{3.18}$$

The reduced density matrix obtained after tracing out Charlie's qubit does not have any effects of noninertial nature and the coherence of the joint state of Alice and Bob is

$$C(\hat{\rho}_{AB}) = 2\sin^2\theta\sin\phi\cos\phi, \tag{3.19}$$

which is the expected standard result. The most common form of the three-qubit W state is the tripartite state of the form $|W\rangle = \frac{1}{\sqrt{3}}(|001\rangle + |010\rangle + |100\rangle)$, and of all the generalized W states it has the maximum amount of coherence and entanglement. In addition, the total coherence and entanglement are distributed in a symmetric manner. The quantum coherence of a tripartite system when Charlie's qubit is accelerated is

$$C(\hat{\rho}) = \frac{4\,\mathrm{Li}_{-1/2}(\tanh^2 r)}{3\cosh r\,\sinh^2 r} + \frac{2}{3}. \tag{3.20}$$

In the $r \to 0$ limit (inertial limit), it reduces to the standard value of $C(\hat{\rho}) = 2$. The change in coherence of the tripartite

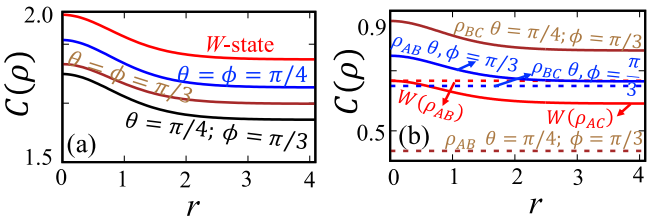

FIG. 5. The variation of quantum coherence as a function of r for fixed values of θ and ϕ is given for (a) the tripartite generalized W state and (b) the two-qubit reduced systems ρ_{AB}, ρ_{BC}, and ρ_{AC}. Here the notation $W(\rho_{AB})$ means the reduced state ρ_{AB} corresponding to the symmetric W state.

generalzed W state is given as a function of the acceleration parameter r for different values of θ and ϕ in Fig. 5(a). From the plots we notice that the quantum coherence is initially maximum at $r = 0$ and then it decreases and reaches a saturation value at large values of r. The decrease in coherence is due to the bifurcation of the Minkowski mode into two Rindler modes, of which one is disconnected from the rest of the system. Any coherence due to this mode is inaccessible to measurements. The saturation value is the amount of accessible coherence, which can never be lost to relativistic motion. The maximal value and saturation value are dependent on the generalization parameter. The $|W\rangle = \frac{1}{\sqrt{3}}(|001\rangle + |010\rangle + |100\rangle)$ state has the maximal coherence at $r = 0$ and also has the maximal saturation value. The quantum coherence of the reduced density matrices of the generalized W state is shown in Fig. 5(b). The quantum coherence of the reduced state $\hat{\rho}_{AB}$ is a constant since the accelerated qubit C has already been traced out. In the case of $\hat{\rho}_{BC}$ we find that the coherence is maximal at $r = 0$ and saturates to a finite value at large accelerations. The curve represents the coherence of $\hat{\rho}_{BC}$ and the dashed lines denote the coherence in the state $\hat{\rho}_{AB}$. In Fig. 6 the contour plot shows the variation of quantum coherence as a function of the generalization parameter θ and ϕ for the acceleration parameters $r = 0.01$ and $r = 4.0$.

Next we look at the case where two qubits, the ones corresponding to Bob and Charlie, are being accelerated. Adopting a similar procedure of replacing the Minkowski states by Rindler modes and tracing out the Rindler second mode, we measure the total quantum coherence of the system. The quantum coherence of the tripartite system is

$$\begin{aligned} C(\hat{\rho}) = {} & 2\sin\theta\cos\theta\sin\phi \\ & \times \frac{\mathrm{Li}_{-1/2}(\tanh^2 r_1)}{\sinh^2 r_1\cosh r_1}\frac{\mathrm{Li}_{-1/2}(\tanh^2 r_2)}{\sinh^2 r_2\cosh r_2} \\ & + 2\sin\theta\cos\theta\cos\phi\frac{\mathrm{Li}_{-1/2}(\tanh^2 r_1)}{\sinh^2 r_1\cosh r_1} \\ & + 2\sin^2\theta\sin\phi\cos\phi\frac{\mathrm{Li}_{-1/2}(\tanh^2 r_2)}{\sinh^2 r_2\cosh r_2}. \end{aligned} \tag{3.21}$$

From Eq. (3.21) we notice that the quantum coherence is a sum of three terms. The first contains the noninertial decoherence from both Bob's and Charlie's qubit. The noninertial contributions from Bob and Charlie appear in the second and third terms, respectively. At the bipartite level, there are two

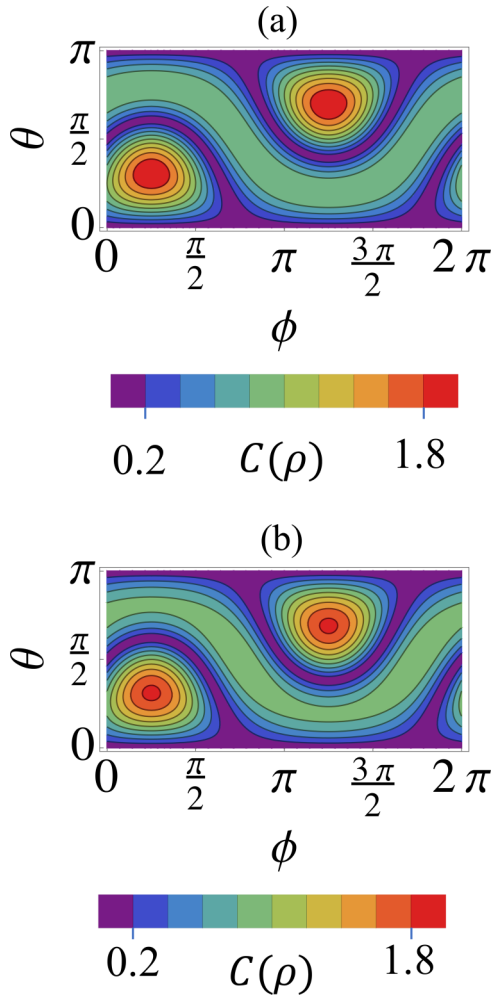

FIG. 6. Contour plot of the quantum coherence $C(\rho)$ as a function of θ and ϕ of the generalized W state when one qubit is in a noninertial frame is shown for (a) $r = 0.01$ and (b) $r = 4.0$.

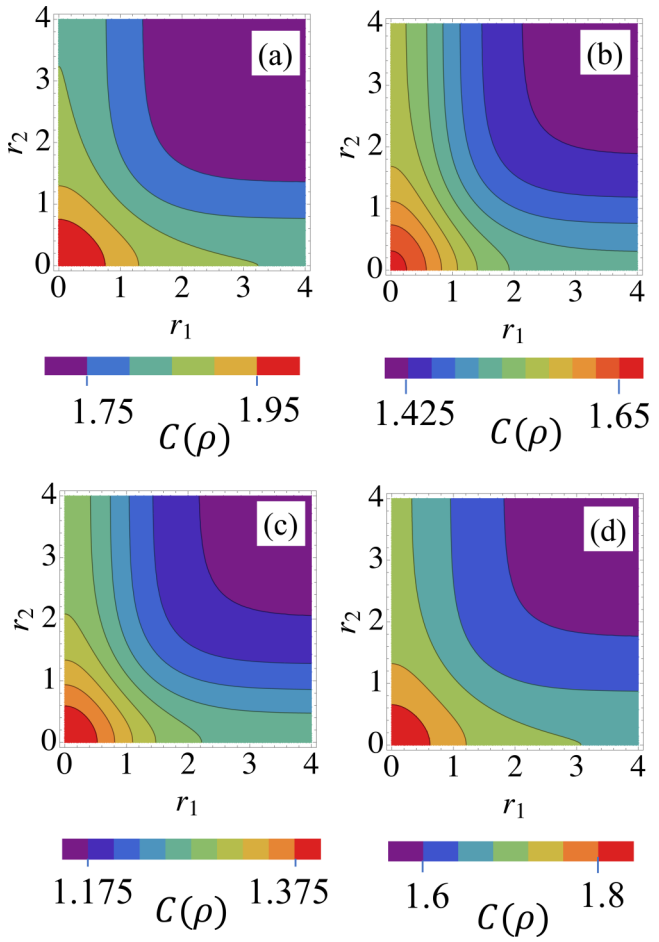

FIG. 7. In the generalized W state when both Bob's and Charlie's qubits are accelerated, the variation of quantum coherence as a function of the acceleration parameters r_1 and r_2 is given for (a) W state; (b) $\theta = \pi/5$, $\phi = \pi/5$; (c) $\theta = \pi/6$, $\phi = \pi/6$; and (d) $\theta = \pi/3$, $\phi = \pi/6$.

possibilities, namely: (i) when Alice's qubit is traced out; (ii) when either Bob's qubit or Charlie's qubit is traced out. The quantum coherence corresponding to these different situations are

$$C(\hat{\rho}_{BC}) = 2\sin\theta\cos\theta\sin\phi\frac{\mathrm{Li}_{-1/2}(\tanh^2 r_1)}{\sinh^2 r_1\cosh r_1} \times \frac{\mathrm{Li}_{-1/2}(\tanh^2 r_2)}{\sinh^2 r_2\cosh r_2}, \tag{3.22}$$

$$C(\hat{\rho}_{AC}) = 2\sin\theta\cos\theta\sin\phi\frac{\mathrm{Li}_{-1/2}(\tanh^2 r_1)}{\sinh^2 r_1\cosh r_1}, \tag{3.23}$$

$$C(\hat{\rho}_{AB}) = 2\sin^2\theta\sin\phi\cos\phi\frac{\mathrm{Li}_{-1/2}(\tanh^2 r_2)}{\sinh^2 r_2\cosh r_2}. \tag{3.24}$$

Here Eq. (3.22) refers to the situation where Alice's qubit is traced out and in the resulting bipartite system both the qubits are in noninertial frames. When Bob's qubit is traced out the total quantum coherence is given through Eq. (3.23), and similarly when Charlie's qubit is traced out Eq. (3.24) gives the quantum coherence of the resulting bipartite state. For the W state of the form $\frac{1}{\sqrt{3}}(|001\rangle + |010\rangle + |100\rangle)$ when both Bob's and Charlie's qubits are accelerated the total quantum coherence of the system is

$$C(\hat{\rho}) = \frac{2}{3}\frac{\mathrm{Li}_{-1/2}(\tanh^2 r_1)}{\sinh^2 r_1\cosh r_1}\frac{\mathrm{Li}_{-1/2}(\tanh^2 r_2)}{\sinh^2 r_2\cosh r_2} + \frac{2}{3}\frac{\mathrm{Li}_{-1/2}(\tanh^2 r_1)}{\sinh^2 r_1\cosh r_1} + \frac{2}{3}\frac{\mathrm{Li}_{-1/2}(\tanh^2 r_2)}{\sinh^2 r_2\cosh r_2}. \tag{3.25}$$

Equation (3.25) reduces to the standard value of $C(\hat{\rho}) = 2$ for $r_1, r_2 \to 0$ and the single-qubit acceleration limit when either r_1 or r_2 tends to zero. In the contour plot shown in Fig. 7 we analyze the variation of the quantum coherence as a function of r_1 and r_2 namely Charlie's and Bob's acceleration parameter for different values of the generalization parameters θ and ϕ. We find that coherence is maximum when r_1 and r_2 are zero and decreases with increase in their value.

A very interesting limiting case of the generalized W state occurs when $\theta = \pi/2$ and $\phi = \pi/4$. The generalized W state corresponding to this value is $(|100\rangle + |010\rangle)/\sqrt{2}$. We can observe that this quantum state is of the biseparable form AB-C, where the AB pair is entangled and C is separable. In this state Charlie's qubit is accelerated, the total quantum

coherence is $C = 1$. This is because the only coherence contribution in the system comes because of the correlation between Alice and Bob's qubit. On the contrary, when Bob is in a noninertial frame of reference, the total quantum coherence in the system is

$$C(\hat{\rho}) = \frac{\mathrm{Li}_{-1/2}(\tanh^2 r)}{\sinh^2 r \cosh r}. \tag{3.26}$$

When both Bob and Charlie are in noninertial frames, the resulting coherence is the same as when Bob is in a noninertial frame. This is because Charlie's qubit does not contribute to the coherence in the system.

For the W state, the tripartite entanglement measured by the π tangle saturates at a finite value [75]. This is in stark contrast with the results obtained for the bipartite entanglement in Ref. [31]. This is again due to the insufficiency in using π tangle as a measure of entanglement. For a W state, the variation of the quantum coherence due to uniform acceleration is similar to the change in the entanglement of the system. However, the ℓ_1 norm measure of coherence is a complete measure, unlike the π-tangle measure of entanglement used in Ref. [75]. The saturation nature of quantum coherence is due to the presence of nonclassical correlations at relativistic velocities. This result holds for single qubit as well as two-qubit accelerated systems.

IV. SEPARABLE STATES

The SLOCC class of classification applies to entangled states. However, in general quantum states may not be entangled. An example of a separable state is $|000\rangle$ and for this state $\hat{\rho} = \hat{\rho}_d$ in the computational basis, and so it is an incoherent state. Here we would like to mention that one of the crucial properties of quantum coherence is that it is a basis-dependent quantity. Hence studying a separable quantum state $|+\!+\!+\rangle$ where $|+\rangle = (|0\rangle + |1\rangle)/\sqrt{2}$ in the σ^z basis we find quantum coherence in the system. To find the relativistic effects, we accelerate either one or two of these qubits. For the accelerated qubits we replace the Minkowski states by their corresponding Rindler modes. We already know that there are two causally disconnected Rindler modes, so we trace out one of the modes and compute the quantum coherence of the rest of the system. Here, when only Charlie's qubit is accelerated, the quantum coherence computed using the ℓ_1-norm measure is

$$C(\hat{\rho}) = 3 + \frac{4\,\mathrm{Li}_{-1/2}(\tanh^2 r)}{\cosh r \sinh^2 r}. \tag{4.1}$$

In the $r \to 0$ limit, the inertial value of the ℓ_1-norm coherence of the system is recovered. When both Charlie's and Bob's qubit are accelerated the quantum coherence is,

$$C(\hat{\rho}) = 1 + \frac{2\,\mathrm{Li}_{-1/2}(\tanh^2 r_1)}{\cosh r_1 \sinh^2 r_1} + \frac{2\,\mathrm{Li}_{-1/2}(\tanh^2 r_2)}{\cosh r_2 \sinh^2 r_2} + \frac{2\,\mathrm{Li}_{-1/2}(\tanh^2 r_1)}{\cosh r_1 \sinh^2 r_1}\,\frac{\mathrm{Li}_{-1/2}(\tanh^2 r_2)}{\cosh r_2 \sinh^2 r_2}. \tag{4.2}$$

From this result, in the appropriate limiting conditions, we can recover the single-qubit result as well as the inertial value.

The coherence measured in the GHZ state, W state, and the separable $|+\!+\!+\rangle$ state is the total amount of quantum coherence present in the states. However, the type of coherence in the GHZ and W states is fundamentally different from the type of coherence present in the $|+\!+\!+\rangle$ state. In the GHZ and W states, the coherence arises due to the correlation between the qubits. Meanwhile the coherence in the $|+\!+\!+\rangle$ state is because of the superposition between the levels within each qubit. These two fundamentally different forms of coherences were identified in Ref. [14]. The coherence arising due to the correlation between the qubits is the global coherence of the system and the coherence resulting from the superposition of the levels within a qubit are called local coherence. These two forms of coherences are complementary to each other in a sense that the increase in the global coherence causes a decrease in the local coherence and vice versa. With an increase in the acceleration the quantum coherence decreases and it saturates at a finite value. To understand this for the $|+\!+\!+\rangle$ state, we can consider the single-qubit $|+\rangle$ system which we can write as

$$|+\rangle = \sum_{n=0}^{\infty} \frac{\tanh^n r}{\sqrt{2}\cosh r}\left(|n\rangle_{\mathrm{I}}|n\rangle_{\mathrm{II}} + \frac{\sqrt{n+1}}{\cosh r}|n+1\rangle_{\mathrm{I}}|n\rangle_{\mathrm{II}}\right). \tag{4.3}$$

Here we can observe that the initial superposition between two levels is spread out between the four modes. Of these two modes corresponding to Rindler region II are traced out and hence there is a loss of superposition and consequently a loss of coherence. This loss is the inaccessible coherence when the system undergoes uniform acceleration.

The GHZ and W states represents one extreme where the global coherence is maximum with zero local coherence and the $|+\!+\!+\rangle$ denotes the other extreme where the local coherence is maximum with no global coherence. However, there are some pure quantum states in which both these types of coherence coexist. For such states we can quantify the global and local coherence using the formula

$$C_G = \|\hat{\rho} - \pi(\hat{\rho})\|_{l_1}, \tag{4.4}$$

$$C_L = \|\pi(\hat{\rho}) - [\pi(\hat{\rho})]_d\|_{l_1}. \tag{4.5}$$

Here $\pi(\hat{\rho}) = \hat{\rho}_1 \otimes \cdots \otimes \hat{\rho}_N$ is the product state of the density matrix $\hat{\rho}$ where the reduced density matrix $\hat{\rho}_1 = \mathrm{Tr}_{(2,\ldots,N)}\,\hat{\rho}$. The quantum state $[\pi(\hat{\rho})]_d$ is the decohered density matrix corresponding to $\pi(\hat{\rho})$ the product state. The total quantum coherence of the system C_T measures coherence contributions from correlations as well as local superpositions. In Ref. [14] a trade-off was observed between the global coherence and local coherence.

V. TRIPARTITE PURE STATES WITH LOCAL AND GLOBAL COHERENCE

In this section we study the noninertial effects when both local and global coherences are present in the system. Towards this end, we analyze the quantum coherence of tripartite $W\bar{W}$ and star states. The $W\bar{W}$ state is a symmetric tripartite state with both local and global coherence. On the contrary the star state is an asymmetric state with both local and global coherences.

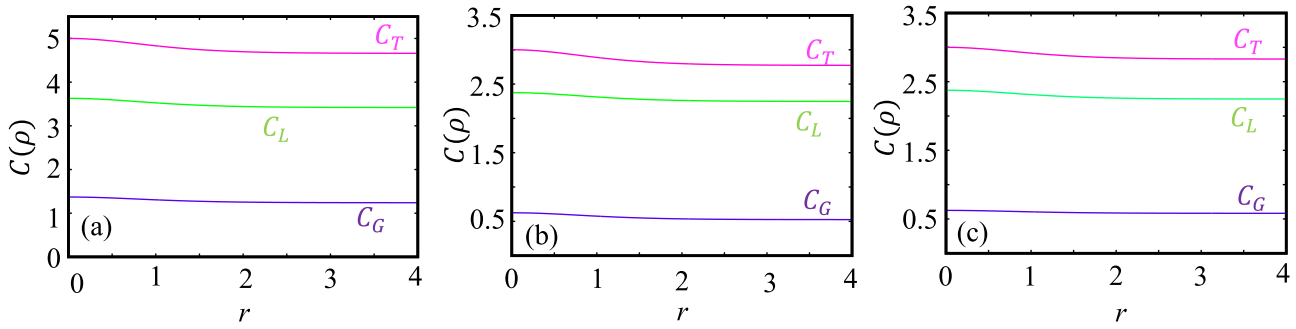

FIG. 8. A plot of the total coherence (C_T), global coherence (C_G), and local coherence (C_L) for (a) the $W\bar{W}$ state, (b) star state when the central qubit is accelerating and (c) star state when the peripheral qubit is accelerating.

A. $W\bar{W}$ state

The three-qubit $W\bar{W}$ state [76] is a linear superposition of the tripartite W state and the $\bar{W}$ state as shown below

$$|W\bar{W}\rangle = \frac{1}{\sqrt{2}}(|W\rangle + |\bar{W}\rangle),$$
$$|W\rangle = \frac{1}{\sqrt{3}}(|001\rangle + |010\rangle + |100\rangle),$$
$$|\bar{W}\rangle = \frac{1}{\sqrt{3}}(|011\rangle + |101\rangle + |110\rangle). \tag{5.1}$$

First, we consider the situation where a single qubit is in a noninertial frame, that is to say only Charlie's qubit is being accelerated. After tracing out one of the Rindler region, the total quantum coherence of the resulting density matrix is

$$C_T(\hat{\rho}) = 2 + \frac{3\,\mathrm{Li}_{-1/2}(\tanh^2 r)}{\cosh r \sinh^2 r}. \tag{5.2}$$

In the $r \to 0$ limit the quantum coherence recovers the inertial limit.

The single-qubit reduced density matrices of the $W\bar{W}$ state in Eq. (5.1) are

$$\hat{\rho}_A = \hat{\rho}_B = \hat{\rho}_C = \begin{pmatrix} \frac{1}{2} & \frac{1}{3} \\ \frac{1}{3} & \frac{1}{2} \end{pmatrix}. \tag{5.3}$$

From the reduced density matrix we notice that the single-qubit state has a finite amount of quantum coherence. Consequently, the product state $\hat{\rho}_A \otimes \hat{\rho}_B \otimes \hat{\rho}_C$ will also have some coherence which is the local coherence of the system. Using Eqs. (4.4) and (4.5) we find the global and local coherence when one of the qubits is in noninertial frame

$$C_G(\hat{\rho}) = \frac{2}{9} + \frac{31\,\mathrm{Li}_{-1/2}(\tanh^2 r)}{27\cosh r \sinh^2 r}, \tag{5.4}$$
$$C_L(\hat{\rho}) = \frac{16}{9} + \frac{50\,\mathrm{Li}_{-1/2}(\tanh^2 r)}{27\cosh r \sinh^2 r}. \tag{5.5}$$

The behavior of the total coherence, global coherence, and local coherence are shown in Fig. 8(a). From the plots we find that all the different forms of coherences show identical behavior, and they decrease with increase in acceleration and attain a saturation value at higher values of acceleration. The results show that both global and local coherence have similar decoherence properties. Hence Unruh decoherence cannot distinguish between the two forms of coherence *viz* the one arising due to the correlations between the qubits and the quantumness due to the superposition between the levels within a qubit.

To study the relativistic effects when two qubits are in noninertial frames, we uniformly accelerate both Bob's and Charlie's qubits. The total quantum coherence of the $W\bar{W}$ state in this scenario is

$$C_T(\hat{\rho}) = \frac{4}{6} + \frac{8\,\mathrm{Li}_{-1/2}(\tanh^2 r_1)}{6\cosh r_1 \sinh^2 r_1} + \frac{8\,\mathrm{Li}_{-1/2}(\tanh^2 r_2)}{6\cosh r_2 \sinh^2 r_2} + \frac{10\,\mathrm{Li}_{-1/2}(\tanh^2 r_1)\,\mathrm{Li}_{-1/2}(\tanh^2 r_2)}{6\cosh r_1 \sinh^2 r_1\ \cosh r_2 \sinh^2 r_2}. \tag{5.6}$$

The total coherence is present as both global coherence arising from interqubit correlations and also as local coherence coming from intraqubit superpositions. The measured values of the global and local coherence of the system are

$$C_G(\hat{\rho}) = \frac{2\,\mathrm{Li}_{-1/2}(\tanh^2 r_1)}{9\cosh r_1 \sinh^2 r_1} + \frac{2\,\mathrm{Li}_{-1/2}(\tanh^2 r_2)}{9\cosh r_2 \sinh^2 r_2} + \frac{25\,\mathrm{Li}_{-1/2}(\tanh^2 r_1)\,\mathrm{Li}_{-1/2}(\tanh^2 r_2)}{27\cosh r_1 \sinh^2 r_1\ \cosh r_2 \sinh^2 r_2}, \tag{5.7}$$
$$C_L(\hat{\rho}) = \frac{2}{3} + \frac{10\,\mathrm{Li}_{-1/2}(\tanh^2 r_1)}{9\cosh r_1 \sinh^2 r_1} + \frac{10\,\mathrm{Li}_{-1/2}(\tanh^2 r_2)}{9\cosh r_2 \sinh^2 r_2} + \frac{20\,\mathrm{Li}_{-1/2}(\tanh^2 r_1)\,\mathrm{Li}_{-1/2}(\tanh^2 r_2)}{27\cosh r_1 \sinh^2 r_1\ \cosh r_2 \sinh^2 r_2}. \tag{5.8}$$

We find that the total coherence, global coherence, and local coherence reduce to their respective inertial values when $r_1, r_2 \to 0$. Also we find that the total coherence is a sum of the global and local coherence for the ℓ_1 norm of coherence.

B. Star state

A star state is an asymmetric quantum state [77,78], so called because a central qubit is entangled with the peripheral qubits collectively, but upon tracing out the central qubit the peripheral ones have a separable form

$$\hat{\rho}_{B,C} = \mathrm{tr}_A(|S\rangle_{A,B,C}\,\langle S|_{A,B,C}) = \hat{\rho}_B \otimes \hat{\rho}_C. \tag{5.9}$$

In the tripartite star state we have a central qubit A which is entangled to other qubits B and C individually. The qubits B and C are not entangled with each other and are referred to as

peripheral qubits. The form of the tripartite star state is

$$|S\rangle = \tfrac{1}{2}(|000\rangle + |100\rangle + |101\rangle + |111\rangle). \tag{5.10}$$

When the central qubit A is accelerated, the total quantum coherence in the system is

$$C_T(\hat{\rho}) = 1 + \frac{2\,\mathrm{Li}_{-1/2}(\tanh^2 r)}{\cosh r \sinh^2 r}. \tag{5.11}$$

The star state has both global coherence and local coherence and they are

$$C_G(\hat{\rho}) = \frac{-1}{4} + \frac{7\,\mathrm{Li}_{-1/2}(\tanh^2 r)}{8\cosh r \sinh^2 r}, \tag{5.12}$$

$$C_L(\hat{\rho}) = \frac{5}{4} + \frac{9\,\mathrm{Li}_{-1/2}(\tanh^2 r)}{8\cosh r \sinh^2 r}. \tag{5.13}$$

When the peripheral qubit B is being accelerated, the total coherence of the system calculated using the ℓ_1 norm of coherence is

$$C_T(\hat{\rho}) = \frac{3}{2} + \frac{3\,\mathrm{Li}_{-1/2}(\tanh^2 r)}{2\cosh r \sinh^2 r}. \tag{5.14}$$

The corresponding global of the system is

$$C_G(\hat{\rho}) = \frac{1}{4} + \frac{3\,\mathrm{Li}_{-1/2}(\tanh^2 r)}{8\cosh r \sinh^2 r}. \tag{5.15}$$

The local coherence of the system on accelerating the peripheral qubit is the same as the local coherence when the central qubit is under acceleration, the expression for which is given in Eq. (5.13). In both the cases, namely when the central qubit and the peripheral qubit are in the $r \to 0$ limit, the results corresponding to the inertial frame are recovered. For the star states, the variation of quantum coherence is qualitatively similar when both the central and peripheral qubits are accelerated. The global local and total coherence have a maximum value in the inertial frame and decrease with acceleration and attain a saturation value for large values of the acceleration, as shown in Fig. 8. From the analysis of the two different situations where either the central qubit or the peripheral qubit is being accelerated, we find that both global and local coherence have similar decoherence properties. This shows that Unruh decoherence affects all kinds of quantumness equally.

Next we look at the situation where two qubits are in noninertial frames of reference. Due to the asymmetry of the star states, there are two possibilities for this situation *viz*: (i) when a peripheral qubit and a central qubit are accelerated; (ii) when both the peripheral qubits are accelerated. The first situation can be analyzed when both Bob's and Charlie's qubits are simultaneously accelerated. The total coherence of the system in this case is

$$C_T(\hat{\rho}) = \frac{1}{2} + \frac{\mathrm{Li}_{-1/2}(\tanh^2 r_1)}{\cosh r_1 \sinh^2 r_1} + \frac{1}{2}\,\frac{\mathrm{Li}_{-1/2}(\tanh^2 r_2)}{\cosh r_2 \sinh^2 r_2} + \frac{\mathrm{Li}_{-1/2}(\tanh^2 r_1)}{\cosh r_1 \sinh^2 r_1}\,\frac{\mathrm{Li}_{-1/2}(\tanh^2 r_2)}{\cosh r_2 \sinh^2 r_2}. \tag{5.16}$$

Under the same conditions the global and local coherence of the star state are

$$C_G(\hat{\rho}) = \frac{1}{2} + \frac{1\,\mathrm{Li}_{-1/2}(\tanh^2 r_1)}{4\cosh r_1 \sinh^2 r_1} - \frac{1\,\mathrm{Li}_{-1/2}(\tanh^2 r_1)}{4\cosh r_2 \sinh^2 r_2} + \frac{5\,\mathrm{Li}_{-1/2}(\tanh^2 r_1)\,\mathrm{Li}_{-1/2}(\tanh^2 r_2)}{8\cosh r_1 \sinh^2 r_1\ \cosh r_2 \sinh^2 r_2}, \tag{5.17}$$

$$C_L(\hat{\rho}) = \frac{1}{2} + \frac{3\,\mathrm{Li}_{-1/2}(\tanh^2 r_1)}{4\cosh r_1 \sinh^2 r_1} + \frac{3\,\mathrm{Li}_{-1/2}(\tanh^2 r_2)}{4\cosh r_2 \sinh^2 r_2} + \frac{3\,\mathrm{Li}_{-1/2}(\tanh^2 r_1)\,\mathrm{Li}_{-1/2}(\tanh^2 r_2)}{8\cosh r_1 \sinh^2 r_1\ \cosh r_2 \sinh^2 r_2}. \tag{5.18}$$

In the second case, when Alice and Bob's qubits are being accelerated, the total coherence of the system is

$$C_T(\hat{\rho}) = \frac{1}{2} + \frac{\mathrm{Li}_{-1/2}(\tanh^2 r_1)}{\cosh r_1 \sinh^2 r_1} + \frac{\mathrm{Li}_{-1/2}(\tanh^2 r_2)}{\cosh r_2 \sinh^2 r_2} + \frac{1}{2}\,\frac{\mathrm{Li}_{-1/2}(\tanh^2 r_1)}{\cosh r_1 \sinh^2 r_1}\,\frac{\mathrm{Li}_{-1/2}(\tanh^2 r_2)}{\cosh r_2 \sinh^2 r_2}. \tag{5.19}$$

The corresponding global and local coherences are

$$C_G(\hat{\rho}) = \frac{\mathrm{Li}_{-1/2}(\tanh^2 r_1)}{4\cosh r_1 \sinh^2 r_1} + \frac{\mathrm{Li}_{-1/2}(\tanh^2 r_2)}{4\cosh r_2 \sinh^2 r_2} + \frac{\mathrm{Li}_{-1/2}(\tanh^2 r_1)\,\mathrm{Li}_{-1/2}(\tanh^2 r_2)}{8\cosh r_1 \sinh^2 r_1\ \cosh r_2 \sinh^2 r_2}, \tag{5.20}$$

$$C_L(\hat{\rho}) = \frac{1}{2} + \frac{3\,\mathrm{Li}_{-1/2}(\tanh^2 r_1)}{4\cosh r_1 \sinh^2 r_1} + \frac{3\,\mathrm{Li}_{-1/2}(\tanh^2 r_2)}{4\cosh r_2 \sinh^2 r_2} + \frac{3\,\mathrm{Li}_{-1/2}(\tanh^2 r_1)\,\mathrm{Li}_{-1/2}(\tanh^2 r_2)}{8\cosh r_1 \sinh^2 r_1\ \cosh r_2 \sinh^2 r_2}. \tag{5.21}$$

All the different quantum coherences attain their inertial values in the limit $r \to 0$. From the expressions of the total, global, and local coherence we find that the $C_T = C_G + C_L$ for all the different cases of star states.

In the tripartite systems like $W\bar{W}$ states and star states, the total coherence in the system is distributed as global and local coherence. Here, by the word global coherence, we mean coherence arising due to all the types of nonclassical correlations (both local and entanglement type) between the qubits. Hence the global coherence does not fall to zero in the infinite acceleration limit and rather saturates to a finite value due to the presence of local correlations. The effect of noninertial motion on local coherence has not been investigated before. From our results we can see that the intraqubit superpositions do not completely vanish in the infinite acceleration limit, which is a very interesting result. In the tripartite systems when either one or two of the parties are in noninertial frames of reference, the accelerated qubits get split into two modes corresponding to the two Rindler regions. The degradation of quantum coherence is because part of the coherence becomes inaccessible to experimental measurement. Both the global and local coherence decay at the same rate. Hence we find that the acceleration affects the interqubit and intraqubit properties in the same manner.

VI. APPLICATIONS

A. Relativistic effects on multipartite state distributed over a network

Let us consider a network of satellites sharing a multipartite quantum state. An important study could be about the effect of acceleration on the quantum coherence of the multipartite system. To understand this, we measure the quantum coherence of the N-partite GHZ and W state. In the N-partite state, we have n number of uniformly accelerated qubits. First let us consider an N-partite GHZ state

$$|\mathrm{GHZ}\rangle = \frac{1}{\sqrt{2}}(|0\rangle^{\otimes N} + |1\rangle^{\otimes N}). \tag{6.1}$$

The total quantum coherence is $C_{\ell_1}(\hat{\rho}) = 1$ for this state. Out of the N qubits if n qubits undergo acceleration, the quantum coherence of the state is

$$C(\hat{\rho}) = \prod_{k=1}^{n} \frac{\mathrm{Li}_{-1/2}(\tanh^2 r_k)}{\sinh^2 r_k \cosh r_k}. \tag{6.2}$$

Let $C_k(\hat{\rho})$ be the quantum coherence of the N-partite system when only the kth qubit is being accelerated. Using this the coherence of the N-partite system with n accelerating qubits can be written as

$$C(\hat{\rho}) = \prod_{k=1}^{n} C_k(\hat{\rho}). \tag{6.3}$$

When all the satellites have the same acceleration, the quantum coherence simplifies to $C(\hat{\rho}) = [C_k(\hat{\rho})]^n$. From this result we can see that the quantum coherence of the N-partite GHZ state falls exponentially with the increase in the number of accelerating satellites. This exponential fall is a manifestation of the genuinely multipartite form of quantum coherence where the loss of even a single qubit makes the state completely incoherent. Hence a small acceleration of each of the m qubits leads to a huge loss of coherence in the entire system. To put this into a numerical perspective let us consider an 11-qubit GHZ state without any of the qubits under acceleration. The quantum coherence of such a system is $C_{\ell_1}(\hat{\rho}) = 1$, and let us consider $r = 2.0$ for each of the qubit. The coherence when only one qubit is accelerating is $C_{\ell_1}(\hat{\rho}) = 0.8988$. Now when ten qubits start accelerating, we can see that the total coherence reduced to $C_{\ell_1}(\hat{\rho}) = (0.8988)^{10} = 0.3439$. For very large values of n, the quantum coherence $C_{\ell_1} \to 0$. Since the reduction of quantum coherence depends on its distribution in a multipartite system, the results obtained here might hold for entanglement as well. This is because coherence and entanglement are distributed in a similar manner. So we can expect entanglement to fall exponentially similarly to quantum coherence. Hence when quantum information is shared between a network of satellites, the quantum coherence is a function of the number of accelerating satellites and the amount of acceleration.

Next we consider the N-partite W state

$$|W\rangle = \frac{1}{\sqrt{N}}(|00\cdots01\rangle + |00\cdots10\rangle + \cdots + |10\cdots00\rangle). \tag{6.4}$$

In the nonrelativistic scenario the total quantum coherence of this state in the noninertial frame of reference is $C_{\ell_1}(\hat{\rho}) = N - 1$. Here if n qubits start accelerating, the quantum coherence of the N-partite state changes to

$$\begin{aligned} C_{\ell_1}(\hat{\rho}) = {} & \frac{2}{N} \sum_{\substack{1 \leqslant i,j \leqslant n \\ i<j}} \frac{\mathrm{Li}_{-1/2}(\tanh^2 r_i)}{\sinh^2 r_i \cosh r_i} \frac{\mathrm{Li}_{-1/2}(\tanh^2 r_j)}{\sinh^2 r_j \cosh r_j} \\ & + \frac{2}{N}(N-n) \sum_{i=1}^{N} \frac{\mathrm{Li}_{-1/2}(\tanh^2 r_i)}{\sinh^2 r_i \cosh r_i} \\ & + \frac{(N-n)[N-(n+1)]}{N}. \end{aligned} \tag{6.5}$$

In the large N limit, when $n \approx N$, the first term which is a product of two polylog functions dominates over the second and the third terms. Hence we would see the quantum coherence falling as a polynomial function of second order. When $n \ll N$ in the large N limit, the third term dominates over the first and second terms. Consequently, the decrease of quantum coherence due to the relativistic effects will be minimal under such situations. If acceleration is the same for all the satellites then we have

$$\begin{aligned} C_{\ell_1}(\hat{\rho}) = {} & \frac{2}{N} \frac{n(n-1)}{2} \left[\frac{\mathrm{Li}_{-1/2}(\tanh^2 r_i)}{\sinh^2 r_i \cosh r_i} \right]^2 \\ & + \frac{2}{N}(N-n)n \left[\frac{\mathrm{Li}_{-1/2}(\tanh^2 r_i)}{\sinh^2 r_i \cosh r_i} \right] \\ & + \frac{(N-n)[N-(n+1)]}{N}. \end{aligned} \tag{6.6}$$

Since the quantum coherence of the N-partite W state is $(N-1)$, it is not possible to compare it with the coherence loss of the GHZ state. To make a comparison between the coherence loss of the GHZ and W states we define

$$C^N_{\ell_1}(\hat{\rho}) = \frac{C^R_{\ell_1}(\hat{\rho})}{C^{NR}_{\ell_1}(\hat{\rho})}, \tag{6.7}$$

where $C^N_{\ell_1}$ is the normalized amount of quantum coherence, $C^R_{\ell_1}$ is the amount of relativistic coherence, and $C^{NR}_{\ell_1}$ is the quantum coherence of the no-relativistic state. For the GHZ state $C^{NR}_{\ell_1} = 1$ and so $C^N_{\ell_1}(\hat{\rho}) = C^R_{\ell_1}(\hat{\rho})$. In the case of the W state, for $r = 2.0$, $C^R_{\ell_1}(\hat{\rho}) = 8.2430$, and $C^{NR}_{\ell_1} = N - 1$. The normalized amount of quantum coherence in the system when 10 out of 11 qubits are being accelerated is $C^N_{\ell_1} = 0.8243$. Hence, for the same number of quantum states and acceleration, we find that the quantum coherence of the W state is more robust to Unruh decoherence when compared with the GHZ state. This implies that, in a multipartite system, sharing quantum coherence in a bipartite manner protects it from decoherence due to relativistic effects.

Figures 9(a) and 9(b) depict the relativistic quantum coherence of the system. In Fig. 9(a) we plot the change in quantum coherence with r for both GHZ and W states. Here we consider two situations where one qubit is being accelerated or ten qubits are being accelerated. In the first case, where one qubit is under acceleration, the loss of coherence is minimal. Compared to the first case, we find that the coherence loss is much higher when ten qubits are accelerated. Also we find that among these states, the W state with increasing accelerating

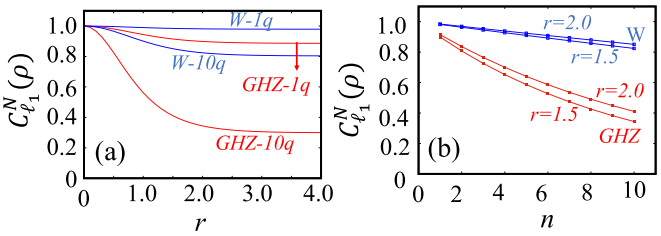

FIG. 9. A plot of the variation of the normalized decoherence (a) with the acceleration parameter r and (b) with the number of accelerated qubits n for a fixed values of $r = 1.5$ and $r = 2.0$. The total number of qubits in the system is $N = 11$.

qubits is more robust to decoherence. In Fig. 9(b) we plot the coherence as a function of the number of accelerating qubits. We find that the loss of coherence is higher with the increase in the number of accelerating qubits. Also, for a given number of accelerating qubits, the GHZ states experience a higher loss of coherence.

B. Coherence degradation at infinite acceleration

The entanglement degradation in the highly relativistic situation was explained in Ref. [31] in the context of a bipartite systems. In Ref. [31], the authors considered the two-qubit case where Alice is an inertial observer and Bob being noninertial with uniform acceleration. In the infinite acceleration limit, noninertial Bob is close to the Rindler horizon, see Ref. [31], which can be considered as the event horizon from the perspective of a black hole. It is well known that a spherical nonrotating static black hole can be described using a Schwarzchild space-time. This can be approximated by the Rindler coordinate in Minkowski space-time in the infinite acceleration limit [79]. Hence, in the existing scenario, we consider Alice and Bob to be close to the event horizon, such that inertial Alice falls into a static black hole and accelerating Bob close to the event horizon escapes from falling into it.

Similarly, our work investigates the quantum coherence degradation in tripartite systems due to relativistic effects. Here we consider three qubits, one each in the possession of Alice, Bob, and Charlie. Degradation of quantum coherence was observed when either a single qubit or two qubits were being accelerated. From our results in Sec. III, for both GHZ and W states we notice a decrease in quantum coherence, but the coherence freezes at a finite amount in the infinite acceleration limit. The entire coherence in the GHZ and W state is due to the correlations between the qubits. In a similar context to understand the relativistic effects on local coherence we study the $|+++\rangle$ separable state. The qualitative behavior of the local coherence in the $|+++\rangle$ state is similar to that of the global coherence of the GHZ and W states. Hence we conclude that, when an inertial observer falls into a black hole, the quantum correlations and quantum superposition shared with the noninertial observer does not vanish completely.

VII. RESULTS AND DISCUSSION

The relativistic effects on the quantum coherence of a multipartite system is investigated using the ℓ_1-norm measure of coherence. Initially, all the qubits are in an inertial frame and can be described using Minkowski space-time coordinates. When some of the qubits are under acceleration, the Minkowski space corresponding to them is divided into two causally disconnected regions. From the Minkowski modes, the Rindler modes can be obtained via the Unruh modes. When we consider a Gaussian Minkowski smearing function it can be approximated by a single Unruh mode. Under the monochromatic approximation we can describe the states using Rindler coordinates in the Minkowski space-time. Hence the quantum coherence initially present in the Minkowski coordinates is distributed between the two Rindler coordinates of which only one is experimentally accessible. The coherence which can be measured in the accessible Rindler region is called the accessible coherence. The coherence corresponding to the other Rindler region is called the inaccessible coherence since it cannot be experimentally measured.

First we investigate the tripartite quantum systems. Based on the SLOCC classification, the tripartite states are classified into the GHZ class and the W classes. For both the GHZ and W states we find that the quantum coherence decreases with the increase in acceleration and attains a saturation value for very high accelerations. Here we note that coherence can exist due to correlations between qubits, which is known as global coherence. Also, coherence may arise due to superposition between the levels within a qubit, referred to as local coherence. The global coherence is the only coherence present in the GHZ and the W states.

Next we consider a separable state of the form $|+++\rangle$ to understand the relativistic effects on local coherence. The local coherence also decreases with the increase in acceleration and saturates at higher acceleration. The local coherence and the global coherence are complementary to each other and the total coherence is a combination of these two types of coherences. Some tripartite quantum states have both local and global coherence. As an example we consider two such quantum states, namely $W\bar{W}$ and star states. In the $W\bar{W}$ state, the global coherence is distributed equally between the three qubits. There is an asymmetric distribution of quantum coherence in the star states. For both these states, all the different forms of coherence, namely the global, local, and total coherence, decreases with an increase in acceleration.

The entanglement of the bipartite system decreases due to relativistic effects and reaches zero in the infinite acceleration limit [31]. However, the tripartite entanglement measured in Ref. [75] using the π tangle does not go to zero for higher values of acceleration. Due to relativistic effects the quantum discord of a system also does not go to zero in the infinite acceleration limit [54]. For the tripartite entanglement, the nonvanishing nature is because the π tangle is not a complete measure of entanglement. However, for the quantum discord this is a fundamental feature of the underlying quantum correlations. From our work we find that there is a qualitative relationship between the total quantum correlations and the quantum coherence of a relativistic quantum system.

In quantum information theory, it is not possible to distinguish between Bell states and the GHZ states through an estimation of entropy. However, we can calculate the quantum coherence of these two states when they are in an inertial frame of reference. Here we again find that $C(|\psi_{\text{Bell}}\rangle) = C(|\psi_{\text{GHZ}}\rangle)$ and so we will not be able to distinguish between

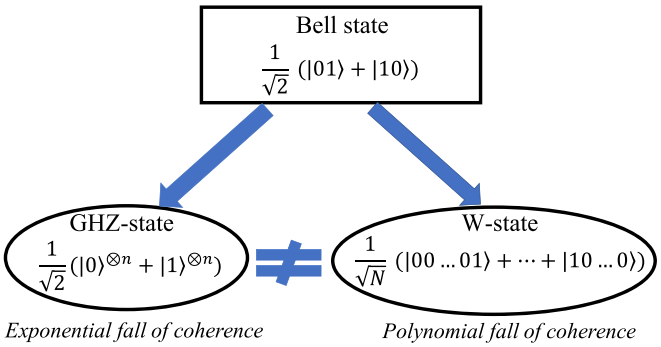

FIG. 10. A schematic illustration of the bifurcation of the Bell state, which displays linear loss of coherence into two extreme classes of states *viz.* GHZ class with exponential loss of coherence and W class with polynomial loss of coherence.

these two states. This is because the GHZ state $\frac{1}{\sqrt{2}}(|000\rangle + |111\rangle)$ can be rewritten as an equivalent Bell state $\frac{1}{\sqrt{2}}(|0\mathbf{0}\rangle + |1\mathbf{1}\rangle)$ where $|\mathbf{0}\rangle = |00\rangle$ and $|\mathbf{1}\rangle = |11\rangle$ are redundantly encoded logical qubits encoding the same quantum information. Next we consider the situation where part of the system is moving with constant acceleration. When the single qubit in GHZ and Bell states moves with constant acceleration it is not possible to distinguish between them. On the contrary when the logical qubit of the GHZ state is in an accelerated motion, then we have $C(|\psi_{\text{Bell}}\rangle) \neq C(|\psi_{\text{GHZ}}\rangle)$ and the reason for this is that the size of the logical qubit under uniform acceleration is bigger than that of the regular qubit of the Bell state. This result is very interesting from a quantum information theory perspective where, in general, we cannot distinguish between Bell and GHZ states or between multipartite GHZ states with a different number of qubits. Nevertheless, a measurement of quantum coherence combined with relativistic motion can differentiate them. Thus the coherence measurement of accelerated systems can be used in quantum-state discrimination.

Next we consider an N-partite GHZ state and W state and estimate the quantum coherence when $n < N$ qubits are accelerated. The GHZ and W states represent the two extremes of coherence sharing. In the GHZ state, the coherence is present in a maximally entangled multipartite manner such that the loss of a single qubit destroys the entire coherence in the system. We find that in a GHZ state with the number of accelerating qubits n increases, thus the coherence falls exponentially. The coherence in a W state is shared in a local bipartite fashion. Here in the case of the W states we observe that the coherence falls polynomially with the increase in the number of accelerating qubits. In Fig. 10, through a flow chart style, we illustrate the quantum coherence decrease as we move from $n = 2$ to $n > 2$ quantum system.

The Bell states describe the maximally entangled states in a two-qubit system. When one of the qubits becomes noninertial, then the coherence of the Bell state is given by $C_{\ell_1} = \text{Li}_{-1/2}(\tanh^2 r)/(\sinh^2 r \cosh r)$. There is only one way to entangle or correlate in a bipartite state. When we move to multipartite systems, there is more than one way to correlate the states. The GHZ and W states denote the two extreme forms of correlation sharing where it is shared in a multipartite fashion in the first case and in a bipartite manner in the later one. When more than one qubit is accelerated, the coherence falls exponentially in the GHZ state and polynomially in the W state. As we move from the bipartite to the multipartite case, the linear fall of coherence observed in Bell-type states changes to an exponential fall for the GHZ states and polynomial decrease for the W state. Hence the Bell-type maximally entangled state clearly bifurcates into two extreme classes of entangled states with exponential fall (GHZ class) and polynomial fall (W state) of coherence. This also proves that the W-state is more robust to Unruh decoherence compared to the GHZ state. This is because the coherence is shared in a genuinely multipartite manner in a GHZ state, but in a W state it is shared only in a bipartite way. For a large N W state, the loss of a few qubits results in a W-like state. This result might be useful for satellite-based quantum communication, where some of the satellites are moving with very high velocities. In Ref. [80] the quantum coherence of multipartite W states for the Dirac field was calculated in terms of the Kruskal modes in certain limiting cases. But in our work, we consider multipartite W states of bosonic modes and compute quantum coherence in a very general setting where an arbitrary number of qubits are being accelerated. In our method the Minkowski modes are converted into Rindler modes in the noninertial frame.

A spherical nonrotating black hole is described by a Schwarzchild space-time. In the infinite acceleration limit, the Schwarzchild space-time can be approximately described by Rindler coordinates in Minkowski space-time. Hence our investigation in the infinite acceleration limit can be used to analyze quantum coherence in the context of black holes. Our study shows that when Alice falls into a black hole, she might still share quantum coherence with Bob and Charlie who are escaping from the black hole. Hence we conclude that quantum correlations and the quantum superposition present in a system do not completely vanish in the relativistic limit.

In our work we use the single-mode approximation where we use single frequency global modes. This can be experimentally realized using localized sources and detectors. Some proposals towards this end might include the use of localized projective measurements [33], homodyne detection [36], and accelerated cavities [81,82]. Here we note that, for a pure state, the l_1-norm measure of coherence is equal to the robustness of coherence [72], which can be directly estimated using the interference of fringes. A possible method is the use of the Berry-phase atomic interferometry experiment [83,84], in which one of the arms of the interferometer is under noninertial motion. The phase difference between the inertial and noninertial arms can give us the change in coherence due to the noninertial motion. Hence an experimental verification of the relativistic effects on quantum coherence might be an interesting future work. On the theoretical side, an investigation on the quantum coherence effects in curved space-time is also an interesting topic to explore.

Note added. Recently, we became aware of the work of the authors of Ref. [85], which independently derived similar results.

ACKNOWLEDGMENTS

C.R. was supported, in part, by a seed grant from IIT Madras to the Centre for Quantum Information, Communication, and Computing. P.R. is funded by an Australian Research Council Future Fellowship (Project No. FT160100397). We are thankful to the anonymous reviewer for their comments on the single-mode approximation, which was very useful.

[1] P. W. Shor, Quantum computing, Documenta Mathematica **1**, 467 (1998).

[2] D. Deutsch and R. Jozsa, Rapid solution of problems by quantum computation, Proc. R. Soc. London A **439**, 553 (1992).

[3] L. K. Grover, A fast quantum mechanical algorithm for database search, *Proceedings of the Twenty-Eighth Annual ACM Symposium on the Theory of Computing* (ACM, New York, 1996), pp. 212–219.

[4] P. W. Shor, Polynomial-time algorithms for prime factorization and discrete logarithms on a quantum computer, SIAM Rev. **41**, 303 (1999).

[5] V. Giovannetti, S. Lloyd, and L. Maccone, Quantum Metrology, Phys. Rev. Lett. **96**, 010401 (2006).

[6] C. H. Bennett, G. Brassard, C. Crépeau, R. Jozsa, A. Peres, and W. K. Wootters, Teleporting an Unknown Quantum State Via Dual Classical and Einstein-Podolsky-Rosen Channels, Phys. Rev. Lett. **70**, 1895 (1993).

[7] D. Bouwmeester, J.-W. Pan, K. Mattle, M. Eibl, H. Weinfurter, and A. Zeilinger, Experimental quantum teleportation, Nature (London) **390**, 575 (1997).

[8] C. H. Bennett and G. Brassard, "Quantum cryptography: Public key distribution and con tos5," in *Proceedings of the International Conference on Computers, Systems and Signal Processing* (IEEE, New York, 1984), pp. 175–179.

[9] C. H. Bennett, F. Bessette, G. Brassard, L. Salvail, and J. Smolin, Experimental quantum cryptography, J. Cryptology **5**, 3 (1992).

[10] J.-D. Bancal, C. Branciard, N. Gisin, and S. Pironio, Quantifying Multipartite Nonlocality, Phys. Rev. Lett. **103**, 090503 (2009).

[11] P. Skrzypczyk, M. Navascués, and D. Cavalcanti, Quantifying Einstein-Podolsky-Rosen Steering, Phys. Rev. Lett. **112**, 180404 (2014).

[12] H. Ollivier and W. H. Zurek, Quantum Discord: A Measure of the Quantumness of Correlations, Phys. Rev. Lett. **88**, 017901 (2001).

[13] T. Baumgratz, M. Cramer, and M. B. Plenio, Quantifying Coherence, Phys. Rev. Lett. **113**, 140401 (2014).

[14] C. Radhakrishnan, M. Parthasarathy, S. Jambulingam, and T. Byrnes, Distribution of Quantum Coherence in Multipartite Systems, Phys. Rev. Lett. **116**, 150504 (2016).

[15] A. Winter and D. Yang, Operational Resource Theory of Coherence, Phys. Rev. Lett. **116**, 120404 (2016).

[16] F. G. S. L. Brandão and G. Gour, Reversible Framework for Quantum Resource Theories, Phys. Rev. Lett. **115**, 070503 (2015).

[17] E. Chitambar and G. Gour, Critical Examination of Incoherent Operations and a Physically Consistent Resource Theory of Quantum Coherence, Phys. Rev. Lett. **117**, 030401 (2016).

[18] E. Chitambar and M.-H. Hsieh, Relating the Resource Theories of Entanglement and Quantum Coherence, Phys. Rev. Lett. **117**, 020402 (2016).

[19] T. Chanda and S. Bhattacharya, Delineating incoherent nonmarkovian dynamics using quantum coherence, Ann. Phys. (NY) **366**, 1 (2016).

[20] C. Radhakrishnan, Z. Lü, J. Jing, and T. Byrnes, Dynamics of quantum coherence in a spin-star system: Bipartite initial state and coherence distribution, Phys. Rev. A **100**, 042333 (2019).

[21] M. Hillery, Coherence as a resource in decision problems: The deutsch-jozsa algorithm and a variation, Phys. Rev. A **93**, 012111 (2016).

[22] C. Zhang, T. R. Bromley, Y.-F. Huang, H. Cao, W.-M. Lv, B.-H. Liu, C.-F. Li, G.-C. Guo, M. Cianciaruso, and G. Adesso, Demonstrating Quantum Coherence and Metrology that is Resilient to Transversal Noise, Phys. Rev. Lett. **123**, 180504 (2019).

[23] J. Ma, Y. Zhou, X. Yuan, and X. Ma, Operational interpretation of coherence in quantum key distribution, Phys. Rev. A **99**, 062325 (2019).

[24] A. Peres and D. R. Terno, Quantum information and relativity theory, Rev. Mod. Phys. **76**, 93 (2004).

[25] J. Dunningham, V. Palge, and V. Vedral, Entanglement and nonlocality of a single relativistic particle, Phys. Rev. A **80**, 044302 (2009).

[26] R. B. Mann and T. C. Ralph, Relativistic quantum information, Class. Quantum Grav. **29**, 220301 (2012).

[27] P. M. Alsing and G. J. Milburn, Lorentz invariance of entanglement, arXiv:quant-ph/0203051.

[28] P. M. Alsing and I. Fuentes, Observer-dependent entanglement, Class. Quantum Grav. **29**, 224001 (2012).

[29] H. Li and J. Du, Relativistic invariant quantum entanglement between the spins of moving bodies, Phys. Rev. A **68**, 022108 (2003).

[30] Y. Shi, Entanglement in relativistic quantum field theory, Phys. Rev. D **70**, 105001 (2004).

[31] I. Fuentes-Schuller and R. B. Mann, Alice Falls into a Black Hole: Entanglement in Noninertial Frames, Phys. Rev. Lett. **95**, 120404 (2005).

[32] D. E. Bruschi, J. Louko, E. Martín-Martínez, A. Dragan, and I. Fuentes, Unruh effect in quantum information beyond the single-mode approximation, Phys. Rev. A **82**, 042332 (2010).

[33] A. Dragan, J. Doukas, E. Martín-Martínez, and D. E. Bruschi, Localized projective measurement of a quantum field in noninertial frames, Class. Quantum Grav. **30**, 235006 (2013).

[34] G.-H. S. . S.-H. D. Qian Dong, and A. J. Torres-Arenas, Tetrapartite entanglement features of w-class state in uniform acceleration, Front. Phys. **15**, 11602 (2020).

[35] W. G. Unruh, Notes on black-hole evaporation, Phys. Rev. D **14**, 870 (1976).

[36] T. G. Downes, T. C. Ralph, and N. Walk, Quantum communication with an accelerated partner, Phys. Rev. A **87**, 012327 (2013).

[37] D. Kabat, Black hole entropy and entropy of entanglement, Nucl. Phys. B **453**, 281 (1995).

[38] L. J. Henderson, R. A. Hennigar, R. B. Mann, A. R. Smith, and J. Zhang, Harvesting entanglement from the black hole vacuum, Class. Quantum Grav. **35**, 21LT02 (2018).
[39] E. Martín-Martínez, L. J. Garay, and J. León, Unveiling quantum entanglement degradation near a schwarzschild black hole, Phys. Rev. D **82**, 064006 (2010).
[40] E. Martín-Martínez, L. J. Garay, and J. León, Quantum entanglement produced in the formation of a black hole, Phys. Rev. D **82**, 064028 (2010).
[41] H. Terashima, Entanglement entropy of the black hole horizon, Phys. Rev. D **61**, 104016 (2000)
[42] E. Verlinde and H. Verlinde, Black hole entanglement and quantum error correction, J. High Energy Phys. 10 (2013) 107.
[43] M. Ahmadi, D. E. Bruschi, C. Sabín, G. Adesso, and I. Fuentes, Relativistic quantum metrology: Exploiting relativity to improve quantum measurement technologies, Sci. Rep. **4**, 1 (2014).
[44] M. Ahmadi, D. E. Bruschi, and I. Fuentes, Quantum metrology for relativistic quantum fields, Phys. Rev. D **89**, 065028 (2014).
[45] Z. Tian, J. Wang, H. Fan, and J. Jing, Relativistic quantum metrology in open system dynamics, Sci. Rep. **5**, 1 (2015).
[46] H. Du and R. B. Mann, Fisher information as a probe of spacetime structure: relativistic quantum metrology in (A) dS, J. High Energy Phys. 05 (2021) 112.
[47] N. Friis, A. R. Lee, K. Truong, C. Sabín, E. Solano, G. Johansson, and I. Fuentes, Relativistic Quantum Teleportation with Superconducting Circuits, Phys. Rev. Lett. **110**, 113602 (2013).
[48] S.-Y. Lin, C.-H. Chou, and B. L. Hu, Quantum teleportation between moving detectors, Phys. Rev. D **91**, 084063 (2015).
[49] P. T. Grochowski, G. Rajchel, F. Kiałka, and A. Dragan, Effect of relativistic acceleration on continuous variable quantum teleportation and dense coding, Phys. Rev. D **95**, 105005 (2017).
[50] J.-I. Koga, G. Kimura, and K. Maeda, Quantum teleportation in vacuum using only unruh-dewitt detectors, Phys. Rev. A **97**, 062338 (2018).
[51] A. G. S. Landulfo, Nonperturbative approach to relativistic quantum communication channels, Phys. Rev. D **93**, 104019 (2016).
[52] K. Kravtsov, I. Radchenko, S. Kulik, and S. Molotkov, Relativistic quantum key distribution system with one-way quantum communication, Sci. Rep. **8**, 6102 (2018).
[53] I. Radchenko, K. Kravtsov, S. Kulik, and S. Molotkov, Relativistic quantum cryptography, Laser Phys. Lett. **11**, 065203 (2014).
[54] A. Datta, Quantum discord between relatively accelerated observers, Phys. Rev. A **80**, 052304 (2009).
[55] E. Jung, M.-R. Hwang, and D. Park, Quantum discord and quantum entanglement in the presence of an asymptotically flat static black hole, Int. J. Quantum. Inform. **11**, 1350061 (2013).
[56] K. Mattle, H. Weinfurter, P. G. Kwiat, and A. Zeilinger, Dense Coding in Experimental Quantum Communication, Phys. Rev. Lett. **76**, 4656 (1996).
[57] R. Ursin, F. Tiefenbacher, T. Schmitt-Manderbach, H. Weier, T. Scheidl, M. Lindenthal, B. Blauensteiner, T. Jennewein, J. Perdigues, P. Trojek *et al.*, Entanglement-based quantum communication over 144 km, Nat. Phys. **3**, 481 (2007).
[58] X.-M. Jin, J.-G. Ren, B. Yang, Z.-H. Yi, F. Zhou, X.-F. Xu, S.-K. Wang, D. Yang, Y.-F. Hu, S. Jiang *et al.*, Experimental free-space quantum teleportation, Nat. Photonics **4**, 376 (2010).
[59] S. Brito, A. Canabarro, D. Cavalcanti, and R. Chaves, Satellite-based photonic quantum networks are small-world, PRX Quantum **2**, 010304 (2021).
[60] S.-K. Liao, W.-Q. Cai, W.-Y. Liu, L. Zhang, Y. Li, J.-G. Ren, J. Yin, Q. Shen, Y. Cao, Z.-P. Li *et al.*, Satellite-to-ground quantum key distribution, Nature (London) **549**, 43 (2017).
[61] J. Yin, J.-G. Ren, H. Lu, Y. Cao, H.-L. Yong, Y.-P. Wu, C. Liu, S.-K. Liao, F. Zhou, Y. Jiang *et al.*, Quantum teleportation and entanglement distribution over 100-kilometre free-space channels, Nature (London) **488**, 185 (2012).
[62] A. Villar, A. Lohrmann, X. Bai, T. Vergoossen, R. Bedington, C. Perumangatt, H. Y. Lim, T. Islam, A. Reezwana, Z. Tang *et al.*, Entanglement demonstration on board a nano-satellite, Optica **7**, 734 (2020).
[63] J. Yin, Y. Cao, Y. H. Li, J. G. Ren, S. K. Liao, L. Zhang, W. Q. Cai, W. Y. Liu, B. Li, H. Dai, M. Li, Y. M. Huang, L. Deng, L. Li, Q. Zhang, N. L. Liu, Y. A. Chen, C. Y. Lu, R. Shu, C. Z. Peng, J. Y. Wang, and J. W. Pan, Satellite-to-Ground Entanglement-Based Quantum Key Distribution, Phys. Rev. Lett. **119**, 200501 (2017).
[64] J. Yin, Y.-H. Li, S.-K. Liao, M. Yang, Y. Cao, L. Zhang, J.-G. Ren, W.-Q. Cai, W.-Y. Liu, S.-L. Li *et al.*, Entanglement-based secure quantum cryptography over 1,120 kilometres, Nature (London) **582**, 501 (2020).
[65] J. Yin, Y. Cao, Y.-H. Li, S.-K. Liao, L. Zhang, J.-G. Ren, W.-Q. Cai, W.-Y. Liu, B. Li, H. Dai *et al.*, Satellite-based entanglement distribution over 1200 kilometers, Science **356**, 1140 (2017).
[66] J. Wang, Z. Tian, J. Jing, and H. Fan, Irreversible degradation of quantum coherence under relativistic motion, Phys. Rev. A **93**, 062105 (2016).
[67] Z. Huang and H. Situ, Quantum coherence behaviors of fermionic system in non-inertial frame, Quant. Info. Proc. **17**, 1 (2018).
[68] J. He, Z.-Y. Ding, J.-D. Shi, and T. Wu, Multipartite quantum coherence and distribution under the unruh effect, Ann. Phys. (Leipzig) **530**, 1800167 (2018).
[69] H.-S. Zeng and H.-M. Cao, Distribution and evolution of quantum coherence for open multi-qubit systems in non-inertial frames, Ann. Phys. (Leipzig) **533**, 2000606 (2021).
[70] S. Rana, P. Parashar, and M. Lewenstein, Trace-distance measure of coherence, Phys. Rev. A **93**, 012110 (2016).
[71] L.-H. Shao, Z. Xi, H. Fan, and Y. Li, Fidelity and trace-norm distances for quantifying coherence, Phys. Rev. A **91**, 042120 (2015).
[72] Y.-T. Wang, J.-S. Tang, Z.-Y. Wei, S. Yu, Z.-J. Ke, X.-Y. Xu, C.-F. Li, and G.-C. Guo, Directly Measuring the Degree of Quantum Coherence using Interference Fringes, Phys. Rev. Lett. **118**, 020403 (2017).
[73] C. Napoli, T. R. Bromley, M. Cianciaruso, M. Piani, N. Johnston, and G. Adesso, Robustness of Coherence: An Operational and Observable Measure of Quantum Coherence, Phys. Rev. Lett. **116**, 150502 (2016).
[74] M. Piani, M. Cianciaruso, T. R. Bromley, C. Napoli, N. Johnston, and G. Adesso, Robustness of asymmetry and coherence of quantum states, Phys. Rev. A **93**, 042107 (2016).
[75] M.-R. Hwang, D. K. Park, and E. Jung, Tripartite entanglement in a noninertial frame, Phys. Rev. A **83**, 012111 (2011).
[76] Sudha, A. R. U. Devi, and A. K. Rajagopal, Monogamy of quantum correlations in three-qubit pure states, Phys. Rev. A **85**, 012103 (2012).

[77] M. Plesch and V. Bužek, Entangled graphs: Bipartite entanglement in multiqubit systems, Phys. Rev. A **67**, 012322 (2003).

[78] M. Plesch and V. Bužek, Entangled graphs. II. Classical correlations in multiqubit entangled systems, Phys. Rev. A **68**, 012313 (2003).

[79] R. M. Wald, *General Relativity* (University of Chicago Press, Chicago, 1984).

[80] S.-M. Wu, Z.-C. Li, and H.-S. Zeng, Quantum coherence of multipartite W-state in a schwarzschild spacetime, Europhys. Lett. **129**, 40002 (2020).

[81] T. G. Downes, I. Fuentes, and T. C. Ralph, Entangling Moving Cavities in Noninertial Frames, Phys. Rev. Lett. **106**, 210502 (2011).

[82] N. Friis, A. R. Lee, D. E. Bruschi, and J. Louko, Kinematic entanglement degradation of fermionic cavity modes, Phys. Rev. D **85**, 025012 (2012).

[83] D. Rideout, T. Jennewein, G. Amelino-Camelia, T. F. Demarie, B. L. Higgins, A. Kempf, A. Kent, R. Laflamme, X. Ma, R. B. Mann *et al.*, Fundamental quantum optics experiments conceivable with satellites-reaching relativistic distances and velocities, Class. Quantum Grav. **29**, 224011 (2012).

[84] E. Martín-Martínez, I. Fuentes, and R. B. Mann, Using Berry's Phase to Detect the Unruh Effect at Lower Accelerations, Phys. Rev. Lett. **107**, 131301 (2011).

[85] S.-M. Wu, H.-S. Zeng, and H.-M. Cao, Quantum coherence and distribution of n-partite bosonic fields in noninertial frame, Class. Quantum Grav. **38**, 185007 (2021).